NTNU – Trondheim
Norwegian University of
Science and Technology

Attenuation of Heave-Induced Pressure Oscillations in MPD

Siri Garli Dragset

Master of Science in Cybernetics and Robotics
Submission date: June 2014
Supervisor: Ole Morten Aamo, ITK

Norwegian University of Science and Technology
Department of Engineering Cybernetics

NTNU
Norwegian University of Science and Technology

Faculty of Information Technology, Mathematics and Electrical Engineering

Department of Engineering Cybernetics

MSC THESIS DESCRIPTION SHEET

Name: Siri Garli Dragset

Department: Engineering Cybernetics

Thesis Title: Disturbance Attenuation in Managed Pressure Drilling

Background

In drilling operations performed in the oil and gas industry it is important to control pressure of the drilling fluid, also called drilling mud. Drilling mud is used primarily for removing cuttings from the well. It is injected at high pressure at the top of the drill string. At the end of the drill string, called the drilling bit, the drilling mud gets into the annulus and then rises together with cuttings up to the surface. At the surface, the cuttings are separated from the mud and the cleaned mud is reinjected into the drill string for further circulation. Apart from removing cuttings from the well, drilling mud is also needed for pressurizing the well. If the pressure in the well is too low, the pressure of the surrounding rock formation can make the well collapse and the drill string gets stuck. At the same time, if the pressure exceeds a certain threshold, it may fracture the well leading to costly consequences. For this reason, it is important to control mud pressure in the well.

In managed pressure drilling (MPD) operations, the well is sealed at the top and the pressure is controlled by opening/closing the valve that releases the mud at the top of the well. This technology has proven successful when drilling from stationary platforms. When drilling from a floater, however, the heaving motion of the floater causes major pressure fluctuations in the well, which must be compensated for using automatic control. An experimental lab facility for testing such control strategies has been built at NTNU. The aim of this project is to demonstrate that attenuation using the choke is feasible. The following points should be addressed by the student:

Tasks:

1) Based on the project work carried out in the fall of 2013, review the modeling and revise if necessary. In particular consider if a more detailed model of the bottom-hole assembly should be included. Verify that any change made to the model improves its predictive capability with respect to the simulator as well as lab data.
2) Revise your control algorithm for the rejection of disturbances based on the new model. Demonstrate its performance in simulations.
3) Check the feasibility of applying your control algorithm in the lab – in particular consider real-time aspects. If not feasible, discuss simplifications and return to point 2).
4) If time permits it, apply your control algorithm in the lab.
5) Write a report.

Supervisor: Professor Ole Morten Aamo

Abstract

The purpose of this thesis is to discuss and perform down-hole pressure management in the well while drilling from a floating rig throughout a pipe connection. Managed Pressure Drilling (MPD) technology has proven successful when drilling from stationary rigs, yet the technology is not used in floaters due to a heave motion caused by waves. It is desirable to retain a constant fluid pressure to prevent well collapses or fractures, which may pose a risk to the employees as well as the environment. In addition, damaged equipment may lead to excessive expenses and production restrictions.

First, a gray-box model to describe the dynamics in the well is derived. As opposed to prior work on the subject, pressure measurements along the drill-string are assumed known and used in the model. The number of measurements in the model identification exceeds the mathematical order of the optimal model of the process. This raises questions concerning over-parameterization. Over-parametrization leads to unnecessary computational load, which should be avoided.

Further, a Model Predictive Controller (MPC) is developed to control the fluid pressure. In order to verify the MPC performance, experiments in three different stages were conducted. Stage 1 was nominal experiments, stage 2 was tests against the Managed Pressure Drilling (MPD) Simulator, and the final stage was tests in the IPT Heave Lab. In the nominal tests, the disturbance was suppressed as much as 80%. Simulator experiments showed positive results as well, and suppressed disturbances from waves with a period of 3 seconds, which is the assumed worst-case scenario, by 63%. The experiments in the IPT Heave Lab were not conducted as planned, thus it was inexpedient to compare the performance to earlier work on the matter.

The disturbance is not observable in practical applications. Thus, it is necessary to predict future disturbances in order for the MPC to account for this. A predictor was implemented based on known down-hole dynamics and it demonstrated good performance in the simulator. Poor performance of the observer in the lab indicated that the parameters in the dynamic equations were not tuned to describe the lab dynamics.

Sammendrag

Denne hovedoppgaven omhandler trykkstyring i oljebrønner i forbindelse med rørtilkobling. Ved boring fra flytende plattform blir trykket direkte påvirket av bølger som hever plattformen. Det er ønskelig å holde trykket konstant, da store trykkforskjeller kan føre til store økonomiske tap og fare for personskader.

Først ble det utviklet en modell som beskriver prosessens dynamikk. Denne er en kombinasjon av en eksperimentell lineær modell og en ulineær grunnprinsippmodell. I motsetning til tidligere forskning er alle trykkmålinger langs borerøret antatt kjent og inkludert i modellen. Det diskuteres om modellen er overparametrisert, da antall målepunkter i systemet er større enn den matematiske ordenen. Overparametrisasjon kan føre til unødvendig høy bruk av regnekraft, og det er foreslått som et punkt i videre forskning å revurdere denne modellen.

Videre ble det designet en modellprediktiv regulator (MPC) for å regulere væsketrykket. Denne ble testet i tre stadier: i nominelle tester, opp mot MPD-simulatoren og i IPT-laben. Regulatoren justerte for forstyrrelser forårsaket av bølger tilfredsstillende i de nominelle testene, med opp til 80% demping. Tester mot simulatoren gav også gode resultater, med 63% demping av forstyrrelser i tilfeller med bølger à periode på 3 sekunder. På grunn av at eksperimenter i laben ikke gikk som planlagt er det uhensiktsmessig å sammenligne resultater fra denne oppgaven med tidligere arbeid.

I praksis er det ikke mulig å måle forstyrrelsen i systemet direkte. Derfor er det nødvendig å forutse fremtidig forstyrrelse, slik at MPC-regulatoren kan ta hensyn til dette. En forstyrrelsesprediktor ble utviklet basert på kjente ulineariteter som beskriver dynamikken nedhulls i brønnen. Prediktoren gav utilfredsstillende resultater i lab, noe som indikerer at parametrene i de kjente ulinearitetene ikke er justert for å beskrive dynamikken i lab.

Preface

This Master's thesis (TTK4900) is written as a part of the Master's program at Department of Engineering Cybernetics in the Spring of 2014. It is a thesis within the specialization field *New Energy, Oil and Gas*, and is a continuation of the project work carried out in the Fall of 2013.

Great thanks goes to my supervisor, Professor Ole Morten Aamo, for giving me help whenever I got stuck, and for being patient with me. Also, big thanks to my fellow students at the office for great motivation and support throughout the whole year. It would have been hard to get up in the morning if it weren't for you!

Special thanks to the ones closest to me. My brother and sister, who have proved that it is possible to get through five years at NTNU and have been great role models to their little sister. My parents, who have always believed in me, even though I haven't quite believed in myself. And my boyfriend who always cheers me up, simply by being around.

Siri Garli Dragset
Thursday 5$^{\text{th}}$ June, 2014

Contents

List of Figures

List of Symbols

g Gravity constant.

h Height.

h_{MPC} Prediction horizon.

ω Wave frequency.

p_c Choke pressure.

p_{dh} Down-hole pressure.

p_i Pressure along drill string, node i.

ρ Fluid density.

v_d Piston velocity, also referred to as the disturbance.

v Manipulated Variable.

System Matrices

A State matrix.

B Input matrix.

C Output matrix.

D Feedthrough matrix.

d Disturbance.

E External input matrix.

u System input.

$\mathbf{x}$ System state.

$\mathbf{y}$ System output.

Subscripts

$(\cdot)_0$ Initial condition.

$(\cdot)_c$ MPC model.

$(\cdot)_d$ Disturbance.

$(\cdot)_{dev}$ Deviation.

$(\cdot)_k$ Kalman filter.

$(\cdot)_L$ Lower bound.

$(\cdot)_m$ Process model.

$(\cdot)_p$ Real process.

$(\cdot)_{ref}$ Reference.

$(\cdot)_U$ Upper bound.

Diacritic Symbols

$\bar{}$ Bar: Stacked matrix or vector.

$\hat{}$ Hat: Estimated parameter.

$\tilde{}$ Tilde: Manipulated matrix or vector.

List of Acronyms

BHA	Bottomhole Assembly.
CV	Controlled Variable.
DSR	Deterministic and Stochastic System Identification and Realization.
DV	Disturbance Variable.
LQR	Linear-Quadratic Regulator.
LTI	Linear Time-Invariant.
MPC	Model Predictive Controller.
MPD	Managed Pressure Drilling.
MV	Manipulated Variable.
NTNU	Norwegian University of Science and Technology.
PI	Proportional-Integrator.
QP	Quadratic Programming.

Chapter 1
Background

1.1 Motivation

Fossil fuels account for a large percentage of today's energy production, making the oil and gas industry a big business worldwide. It is desirable to develop technology that increases the oil production. An increase is achievable by discovering new oil deposits, in addition to accessing wells that earlier have not been commercially viable. There are several causes to inaccessibility, among them narrow drilling windows. The drilling window is the desired pressure region to remain within during drilling. It is

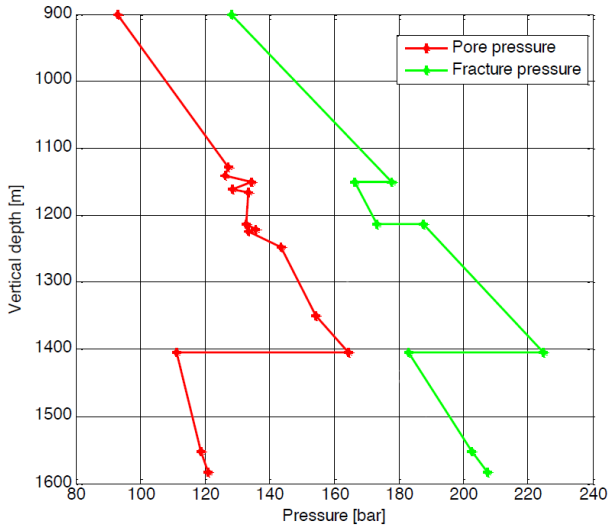

Figure 1.1: Drilling window in a well. Courtesy of Statoil

refined by the pore pressure, which is the pressure of the fluids within the rock pores

surrounding the hole, and the fracture pressure, which is the pressure inside the well that would fracture the bore-hole, demonstrated in figure 1.1. According to figure 1.1, it is necessary to drill through the narrow window at 1400 meters depth in order to access reservoirs deeper in the well.

Violation of the pressure margin can trigger well collapses or "kicks". If the pore pressure exceeds the pressure inside the well, the rock pores may break and cause the fluids to flow into the well-bore. This might cause a kick or a fatal blow-out. Furthermore, if the pressure inside the well exceeds the fracture pressure, the pores might collapse, resulting in damaged reservoirs, well and equipment. Pressure control is therefore an important issue[2].

MPD - Managed Pressure Drilling

Managed Pressure Drilling (MPD) is the term used for operations where the top of the well is sealed, and the IADC defines it as follows[13]:

> Managed Pressure Drilling (MPD) - an adaptive drilling process used to precisely control the annular pressure profile throughout the wellbore. The objectives are to ascertain the downhole pressure environment limits and to manage the annular hydraulic pressure profile accordingly
> *- IADC, International Association of Drilling Contractors*

To impose pressure in the well, drilling mud[1] is injected through a pump at the top of the well. The pressure is then controlled by discharging the mud through a valve at the outlet of the annulus at a certain rate. Figure 1.2 shows a sketch of the outline of the MPD concept.

When drilling from a stationary rig, this technology has proven successful. It is because the stationary rig will not move significantly during drilling. However, a floating rig will have vertical movements due to waves. This movement is known as the *heave motion*. The down-hole pressure in the well is strongly affected by the heave motion when drilling from a floater, and it is therefore desirable to compensate for this using automatic control. MPD from floating rigs is currently not used in practical applications, and the objective is to examine the possibilities of this.

[1] Drilling mud is a mixture of clay, fluids and chemicals used primarily to remove cuttings from the well and to cool the drilling bit during operation. The fluid dynamics are not considered in this project.

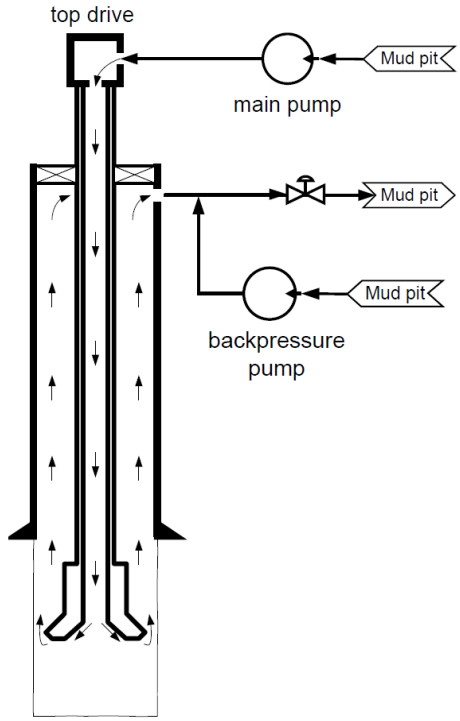

Figure 1.2: Oil rig using MPD. The well is sealed, and the drilling mud is discharged through a valve. Courtesy of Statoil

1.2 Thesis Overview

The aim of this thesis is to develop a control algorithm to reject disturbances from the heave motion on a floating rig during MPD. In the spring 2013, Anders Albert wrote a Master's thesis on the subject. First, a model of the process was identified using black-box identification. The model was identified from experimental data from the lab, with the choke pressure and the piston velocity as input, and measurement of the down-hole pressure as output[2]. This model was then used in the development of a model predictive controller with feedforward of the disturbance[3]. The controller's ability to reject disturbance was shown in the IPT Heave Lab.

The disturbance was assumed known in Albert's setup. In practical applications, the piston velocity is not known, and it is currently not possible to obtain measurements of this. Thus, this measurement is not included in the process model.

[2]For more details about the model identification, see chapter 2.
[3]The disturbance is the piston velocity, which causes pressure changes in the well.

Consequently, a prediction is needed, and an observer is implemented to substitute for the measurement.

Further, changes are done in the setup for the model identification. A gray-box model is identified instead of a pure black-box model, with the assumption that measurement from pressure nodes along the drill-string is available. Because these measurements are not available in current equipment in wells, it is of interest to examine if these measurements improve the controller performance.

With these changes, a new control algorithm is developed to reject the wave impact on the fluid pressure in the well.

1.3 Objectives of the Thesis

In the thesis description, the following points are specified:

1. Based on the project work carried out in the Fall of 2013, review the modelling and revise if necessary. In particular consider if a more detailed model of the bottom-hole assembly should be included. Verify that any change made to the model improves its predictive capability with respect to the simulator as well as lab data.
2. Revise the control algorithm for the rejection of disturbances based on the new model. Demonstrate its performance in simulations.
3. Check the feasibility of applying your control algorithm in the lab – in particular consider real-time aspects. If not feasible, discuss simplifications and return to point 2.
4. If time permits it, apply the control algorithm in the lab.

1.4 Outline of the Report

The report is structured in the following way: In the first chapter, the background and motivation for the thesis is stated. Also, the thesis description are defined.

The chapters 2-4 constitute the theory part of the thesis. Chapter 2 explains the procedure of deriving a mathematical model for the process. Each of the blocks in figure 1.3 are described. Chapter 3 discusses the state observer design, and chapter 4 concerns the theory behind the Model Predictive Controller. The need of an observer

is established in advance, thus the observer design is described prior to the controller design.

Chapter 5 and 6 concern the MPD Simulator and the IPT Heave Lab, including the conducted tests. Chapter 7 presents and discusses the results, and chapter 8 contains the conclusion and proposals for further work.

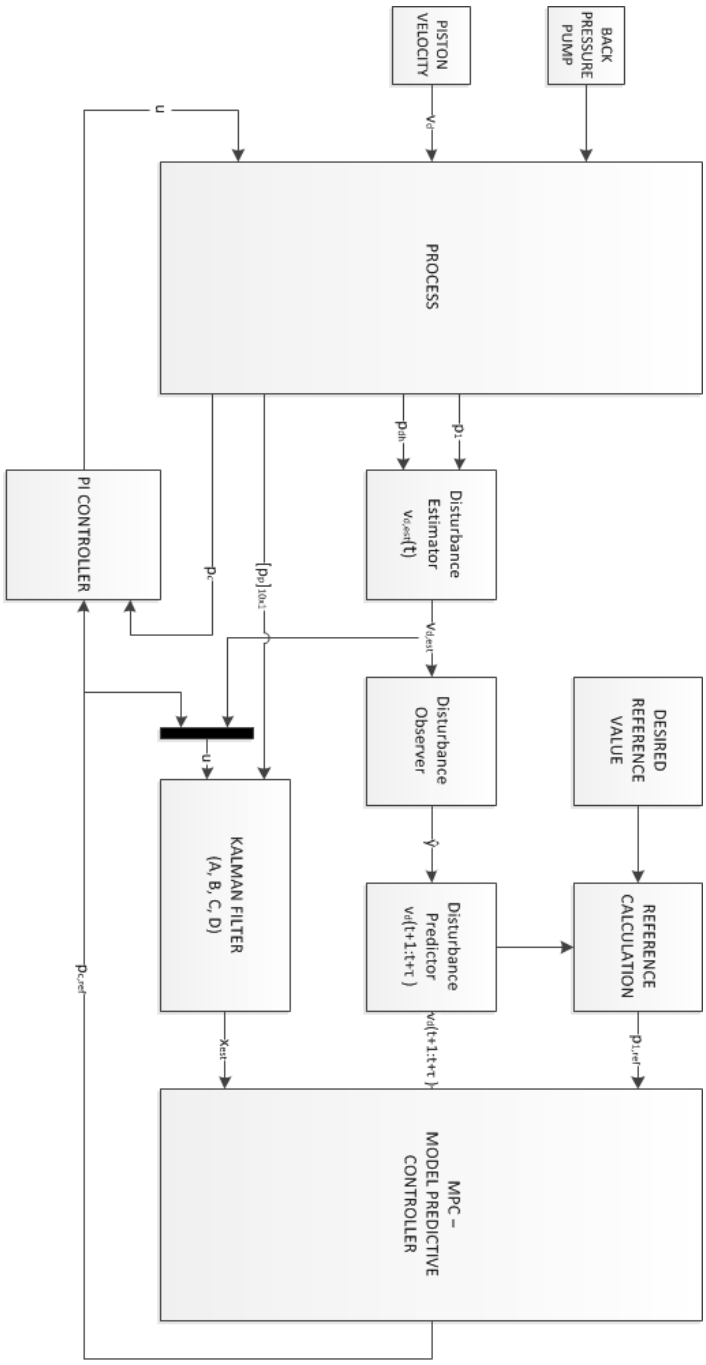

Figure 1.3: This block diagram shows the outline of the system implementation.

Chapter 2
Model Identification

Model Predictive Controller (MPC) is used to control the down-hole pressure in the well. This controller is, as the name implies, based on predictions of future behavior of the system. A model describing the process dynamics is needed to obtain the predictions. This model processes current measurements and Manipulated Variables (MVs) and predicts the state of the system in the next time step. The MPC then adjusts its Controlled Variable (CV) according to these predictions. In the project work carried out in the fall of 2013 [4], a *non-linear first principles* model and a *linear experimental* model were considered. Based on these considerations, a combination is introduced. Figure 2.1 shows the relationship between the different model categories.

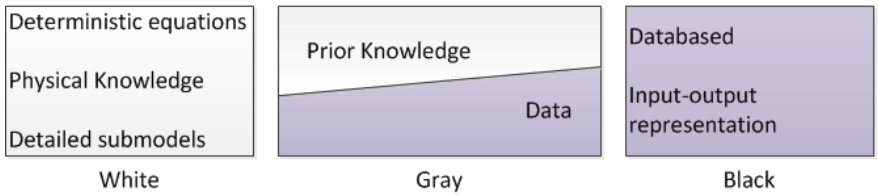

Figure 2.1: This figure shows properties of the model categories. White areas represent the non-linear first principle model, while the purple areas represent the linear experimental model.

First principle models, known as white-box models, are derived from mass and energy balance equations, i.e. describing the system based on well established laws of physics. The non-linear approach requires a wide insight into the physical system, and a great amount of development work is required. In addition, the physics in

most systems are to some extend unknown, it can therefore be hard to derive a satisfactory model based on this.

White-box models are advantageous for describing systems with comprehensive non-linear dynamics. Furthermore, if a model can be used in several process units, it is beneficial to embed the extra amount of work to derive a good physical description rather than approximating the process with a *Linear Experimental Model*, known as the black-box model.

The black-box model identification method creates a model by data-fitting. It takes a set of known input and output data and builds a model which resemble their behavior. Known dynamics are not taken into account. Consequently, none of the equations refer to specific dynamics in the process. Thus, the model generated can be viewed as a black box where only input and output is known, while knowledge about the model equation structure is extraneous.

Gray-Box Modelling

The non-linear first principles model is a convenient alternative because the process is already well explored. Nevertheless, the linear experimental model has an advantage in its simplicity. This approach to the modeling challenge is extensively used in practical cases as it is easily obtained. By combining these two model identification methods, both the simplicity of the black-box modeling and the utilization of known dynamics from the first principal modeling are exploited. Thus, a gray-box method is used for system identification. Known dynamics from the down-hole of the well are utilized in the system definition, while the dynamics from the drill string are assumed unknown. For complementary information about different model representations, see Hauger's lecture notes [7].

2.1 Black-Box Modeling

2.1.1 Procedure

Black-box modeling is based on comparison between known behavior of a real process and behavior of different experimental models. The experimental models are created by applying input signals with known expected output from the process to a set of linear equations of a specified mathematical order. The data is fitted as closely as possible to the expected output to obtain a sufficiently accurate model.

Figure 2.2 shows the inputs and outputs available to the identification of the unknown dynamics conducted:

$$\mathbf{u}_m = [p_c \; v_d]^T \tag{2.1}$$

$$\mathbf{y}_m = [p_1 \; p_2 \; p_3 \; p_4 \; p_5 \; p_6 \; p_7 \; p_8 \; p_9 \; p_{10}]^T \tag{2.2}$$

p_c is the pressure at the choke inlet and v_d is the piston velocity[1]. The latter is the disturbance in the real system, and follows the vertical movement of the waves in the ocean. $p_1 - p_{10}$ are pressure node measurements along the inside of the drill-string. It is discussed in the result chapter, chapter 7, whether it is advantageous to include all the pressure measurements $p_1 - p_{10}$ in the identification.

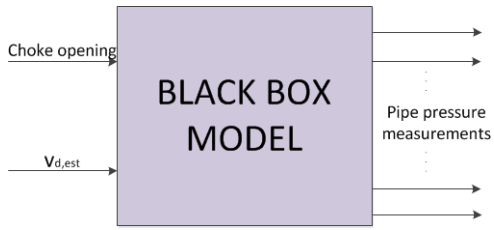

Figure 2.2: Black-box representation of the process model

The model identification is done around the operating point of the process, i.e. the operation point value is subtracted from the measurements. This emphasizes the rate of change.

The deviation between the outputs from the real and the modeled process is the measure of accuracy of the experimental model. The deviation is calculated as an root-mean-square deviation, as shown in equation 2.3.

$$\text{RMSE} = \sqrt{\frac{\sum_{i=1}^{k}(\hat{y}_i - y_i)^2}{k}} \tag{2.3}$$

If the deviation is sufficiently small, the mathematical model found by the black-box approximation can be considered adequate.

2.1.2 Identification Data

It is important to generate a sufficiently *rich* input signal when performing system identification. If this is not fulfilled, it is unlikely to achieve parameter convergence.

[1]Piston is the collective term of the bottom-hole assembly, which consists of the drill bit and other equipment used at the bottom of the well.

A rich input signal varies sufficiently to excite the system. A combination between sinusoidal waves with various periods and amplitudes, and random signals was used in the identification to ensure parameter convergence.

2.1.3 Algorithm

The algorithm used to generate the previously mentioned state space system is called the Deterministic and Stochastic System Identification and Realization (DSR). The purpose of DSR is to estimate the state space system matrices on the form given by equation 2.4. This algorithm was developed by David Di Ruscio [3], and is a subspace approach based on observations.

$$\begin{aligned} \mathbf{x}_m(k+1) &= \mathbf{A}_m\mathbf{x}_m(k) + \mathbf{B}_m\mathbf{u}_m(k) + \mathbf{E}_m\mathbf{e}_m(k), \quad \mathbf{x}_m(k=0) = \mathbf{x}_0 \\ \mathbf{y}_m(k) &= \mathbf{C}_m\mathbf{x}_m(k) + \mathbf{D}_m\mathbf{u}_m(k) + \mathbf{e}_m(k) \end{aligned} \tag{2.4}$$

The system matrices $\mathbf{A}_m$, $\mathbf{B}_m$, $\mathbf{C}_m$ and $\mathbf{D}_m$ represents the process model. $\mathbf{e}_m$ is the innovation, the difference between the optimal predicted and the observed value of the output. The optimal Kalman filter gain matrix is calculated from the algorithm as well. The Kalman filter is discussed in section 3.4.

2.2 White-Box Modeling

The known down-hole dynamics is describing the piston velocity in the terms of pressure change in the well. It is assumed that the disturbance is not measurable, thus it is necessary to make an estimate of the piston velocity, $\hat{v}_d$. This is done by solving equation 2.5 with respect to v_d. The measurements of p_1 and p_{dh} is available, thus the only unknown variable in equation 2.5 is v_d. Figure 2.3 shows the connection between the pressure nodes in the piston compartment.

$$p_{dh} - p_1 = f_{d,1}v_d + f_{d,2}v_d|v_d| + \rho g h \tag{2.5}$$

The two coefficients $f_{d,1}$ and $f_{d,2}$ are known, identified in Aanestad's Master's thesis [11]:

$$f_{d,1} = -43840 \left[\frac{\text{Pa s}}{\text{m}}\right]$$
$$f_{d,2} = -410400 \left[\frac{\text{Pa s}}{\text{m}}\right]$$

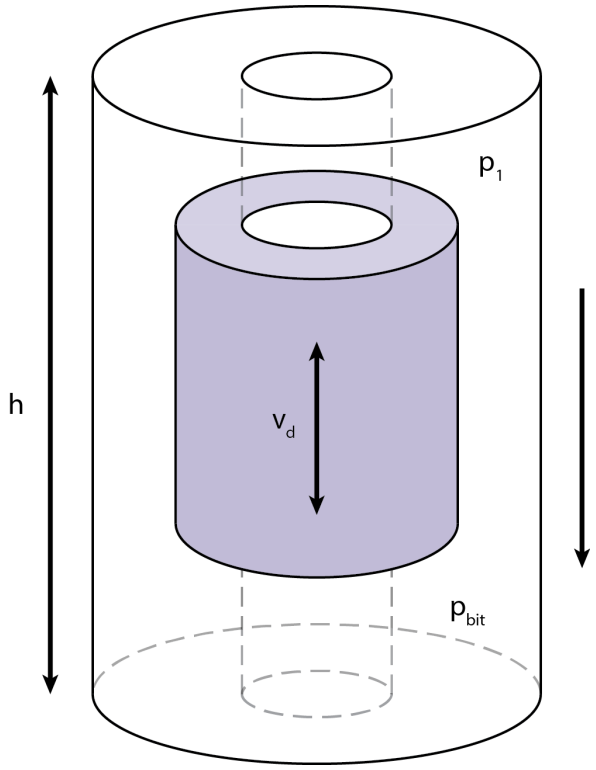

Figure 2.3: The piston (colored) moves vertically in the compartment, and this affects the pressure in the well.

Chapter 3
Observer Design

As discussed in the previous chapter, non-linear dynamics from the well are thoroughly studied and taken into account, in particular, the down-hole dynamics. Figure 2.3 shows the piston compartment and the relationship between the down-hole pressure and the pressure node closest to the down-hole node. This relationship is explained more closely in this chapter.

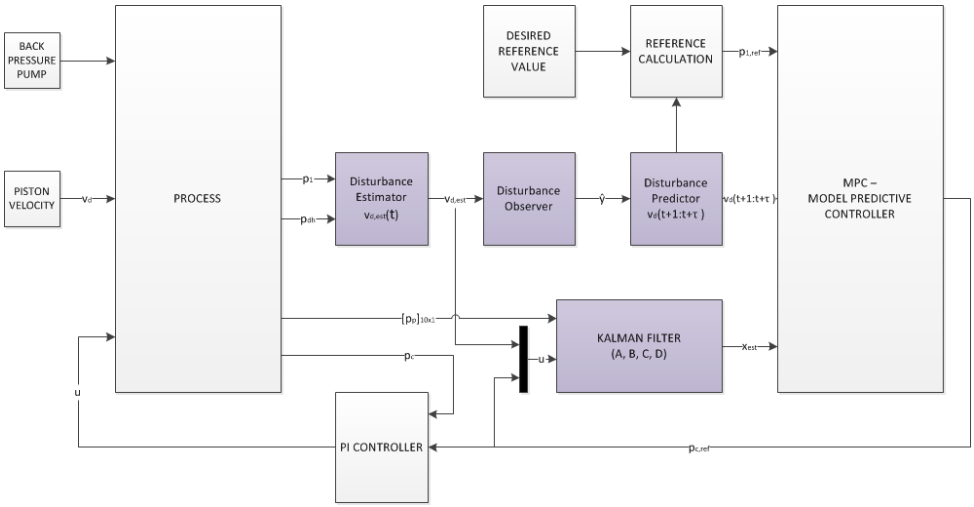

Figure 3.1: This block diagram shows the schematic setup of the control system. The colored blocks in the diagram represents the disturbance estimation and prediction part of the system.

In addition to the disturbance estimation, this chapter concerns the prediction of the future disturbance, and the state observer design. Figure 3.1 shows an overview

of the implemented system, and the connection between different elements.

3.1 Disturbance Estimation

In the well, the piston movement caused by waves has a great impact on the down-hole pressure. When the piston moves downwards, the volume beneath the Bottomhole Assembly (BHA) decreases, creating a pressure increase. Similarly, the pressure drops when the BHA moves upwards. It is desirable to procure an estimate of the piston velocity in order to predict future pressure changes in the well.

By solving equation 2.5 with respect to the piston velocity, v_d, an estimation of the current piston velocity is obtained. This results in a quadratic equation, which normally has two solutions. However, the absolute value sign in the quadratic term gives the equation four possible solutions. To know which of the possible solutions to choose, analysis of the equation is needed.

$$f_{d,2}v_d|v_d| + f_{d,1}v_d + \rho gh - (p_{dh} - p_1) = 0 \tag{3.1}$$

The equation is simplified by defining the following:

$$F = \frac{f_{d,1}}{f_{d,2}}$$
$$K_d = \frac{\rho gh - (p_{dh} - p_1)}{f_{d,2}}$$

By looking closer at the equation, it is clear that a negative K_d gives a positive $\hat{v}_d$, and vice versa. This gives the two equations:

$$\hat{v}_d^2 + F\hat{v}_d + K_d = 0 \tag{3.2}$$
$$\hat{v}_d^2 - F\hat{v}_d - K_d = 0 \tag{3.3}$$

Solving these equations gives the following solutions:

$$\hat{v}_d = \begin{cases} \frac{-F+\sqrt{F^2-4K_d}}{2} & \text{if } K_d \leq 0 \\ \frac{F-\sqrt{F^2+4K_d}}{2} & \text{if } K_d > 0 \end{cases} \tag{3.4}$$

As mentioned, a negative K_d gives a positive velocity, and a positive K_d gives a negative velocity. By utilizing this, it is clear that there only exists one possible solution for $\hat{v}_d$ at any time.

3.2 Disturbance Prediction

3.2.1 Observer Design

It is known that waves cause heave motion of the floating rig, which consequently leads to oscillations in the down-hole pressure in the well. The relationship between the waves and the pressure oscillations are well studied and by utilizing this, an observer can be obtained. The disturbance observer provides an estimate of the internal state of the disturbance, calculated from the estimate of the current piston velocity.

The disturbance is modeled as a harmonic wave which can be described as follows:

$$v_d(t) = a\sin(\omega t + \phi) \tag{3.5}$$

Defining the following gives the state space representation in equations 3.6-3.7:

$$\begin{aligned} x_{d,1}(k) &= v_d(k) = y_d(k) \\ x_{d,2}(k+1) &= \omega x_{d,2}(k) \\ x_{d,2}(k+1) &= -\omega x_{d,1}(k) \end{aligned}$$

$$\mathbf{x}_d(k+1) = \begin{bmatrix} x_{d,1}(k+1) \\ x_{d,2}(k+1) \end{bmatrix} = \begin{bmatrix} 0 & \omega \\ -\omega & 0 \end{bmatrix} \mathbf{x}_d(k) \tag{3.6}$$

$$\hat{y}_d(k) = \begin{bmatrix} 1 & 0 \end{bmatrix} \mathbf{x}_d(k) \tag{3.7}$$

By performing pole placement, the loop is closed, and the poles of the closed-loop system is placed in pre-determined locations to ensure stability. In this case, the poles are placed in the left half plane.

$$\begin{aligned} \mathbf{x}_d(k+1) &= \mathbf{A}_d\mathbf{x} + \mathbf{L}(y_d(k) - \hat{y}_d(k)) \\ \hat{y}_d(k) &= \mathbf{C}_d\mathbf{x}_d \end{aligned} \tag{3.8}$$

3.2.2 Prediction

Next, the current state of the disturbance from the disturbance observer is used to calculate the prediction of the future disturbance $v_d(k+1 \rightarrow k+h_{MPC})$. This is done by simulating the system in equations 3.6-3.7 with the current state of the disturbance as initial value. This is implemented in Simulink as a level-2 S-function in Matlab[10].

3.3 Reference Pressure Prediction Calculation

The aim of this thesis is to control the down-hole pressure, p_{dh}, to follow a reference pressure. This reference is set by the user of the system, and can be both constant and varying.

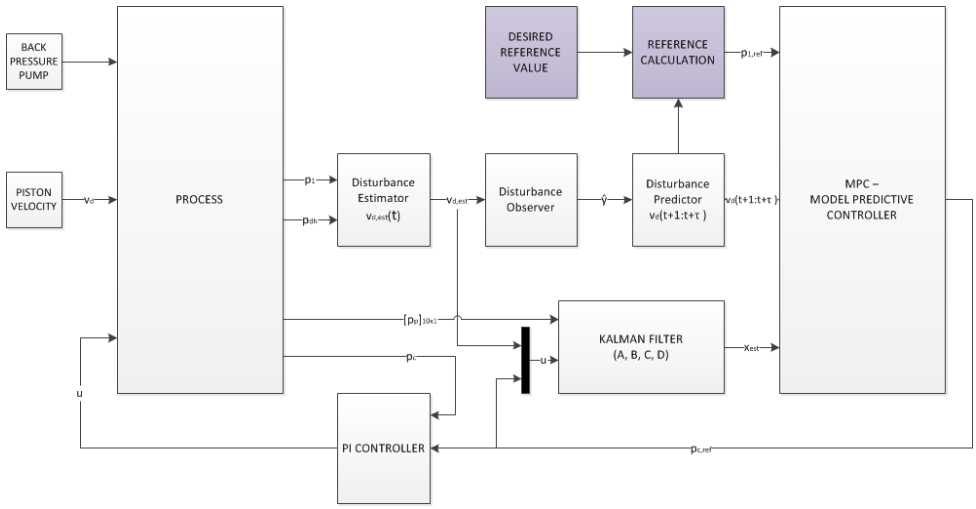

Figure 3.2: The reference calculation occurs in the coloured block.

As explained in chapter 4.1, the optimization problem is formulated to minimize the pressure deviation between the predicted value and the reference value. The MPC uses the black-box model of the process as a base for its internal model. Since the down-hole pressure is not included in this model, it can not be controlled directly by the MPC. Instead, it is expedient to use the known relationship between p_{dh} and p_1 to find a reference pressure $p_{1,ref}$ which corresponds to the desired $p_{dh,ref}$ to feed-forward to the MPC. Equation 3.9 is used to calculate $p_{1,ref}$:

$$p_{1,ref} = p_{dh,ref} - f_{d,1}\hat{v}_d - f_{d,2}\hat{v}_d|\hat{v}_d| - \rho g h \tag{3.9}$$

By using the disturbance prediction over the prediction horizon h_{MPC}, a reference trajectory for $p_{1,ref}$ over the horizon can be obtained by once again utilizing equation 3.9. Figure 4.4a shows a constant p_{dh} reference trajectory and the corresponding oscillating p_1 reference trajectory is shown in figure 4.4b.

3.4 The Kalman Filter

The MPC is a state feedback controller. In this case, the internal state of the process is not known, thus it needs to be estimated. The Kalman Filter is an optimal state estimator that uses a mathematical model to estimate future internal states of a process, and is applicable to stochastic processes. These estimates is used as the actual states by the controller. Algorithm 4.1 explains the process progress.

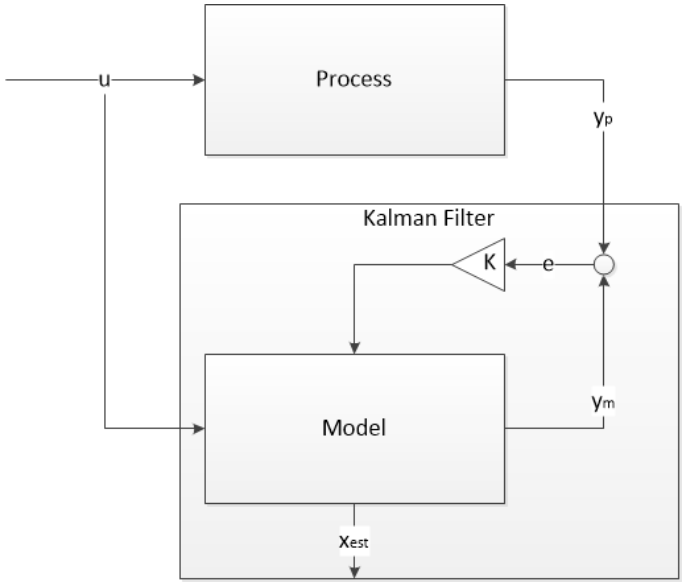

Figure 3.3: Block diagram that shows the concept of the Kalman Filter.

Equations 3.10-3.11 describe the observer in mathematical terms. The model from the black-box identification in chapter 2.1 is used to estimate the future internal state.

$$\hat{\mathbf{x}}_m(k+1) = \mathbf{A}_m\hat{\mathbf{x}}_m(k) + \mathbf{B}_m\mathbf{u}_m(k) + \mathbf{K}_K(\mathbf{y}_m(k) - \mathbf{y}_p(k)) \tag{3.10}$$

$$\mathbf{y}_m(k) = \mathbf{C}_m\hat{\mathbf{x}}_m(k) + \mathbf{D}_m\mathbf{u}_m(k) \tag{3.11}$$

Here, $\mathbf{y}_m$ is the estimated output given by the model, while $\mathbf{y}_p$ is the process output. The optimal Kalman gain $\mathbf{K}_K$ is calculated in the model identification by the *dsr*-algorithm. Since the system is an Linear Time-Invariant (LTI)-system, the Kalman gain is time-invariant, i.e. constant.

Some requirements need to be fulfilled in order to apply the Kalman filter. At least one physical measurement ($\mathbf{y}_p$) needs to be available, and the input u must be applied to both the real system and the model. Both the down-hole pressure measurement and the pressure measurements along the drill string are available in this project. Although this may not be a realistic setup, it is possible using the simulator or the IPT heave lab. It can be seen from figure 3.2 that the input $\mathbf{u}$ is applied to both the real process and the model[1].

[1]Remark that the input $\mathbf{u}_p$ is transposed from being a choke pressure reference to a choke opening reference. This is explained in chapter 4

Chapter 4

MPC - Model Predictive Control

After identifying a dynamic process model, the next step is to design a controller. In an advanced control system, it is not always sufficient with a conventional, relatively simple controller, such as an Linear-Quadratic Regulator (LQR). For example, if the set-point for a control process changes over time, it is advantageous to include a more advanced process control to calculate and apply this.

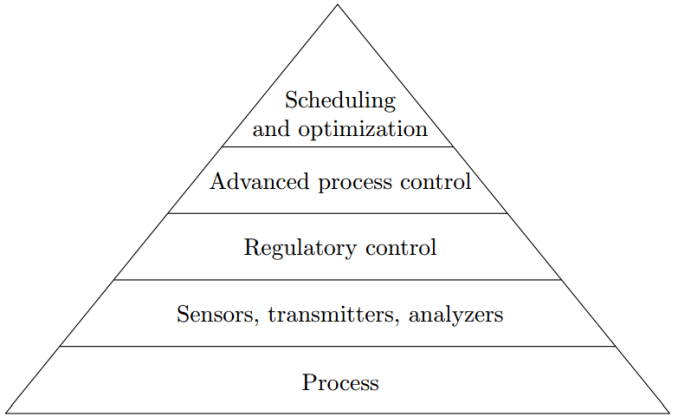

Figure 4.1: Process control hierarchy. The advanced control layer contains the MPC. Figure obtained from lecture notes[6].

Figure 4.1 shows an overview of the hierarchy in a control system. The process communicates with the regulatory control layer by transmitters and sensors in the overlying layer. The regulatory control layer performs simple control according to what the Advanced Process Controller (APC) commands. The MPC is located in the APC layer.

In the well, the propagation of pressure changes along the drill string causes a delay from the desired pressure is applied until it actually is achieved. This causes requirements of prediction in the controller, and this is a reason why the MPC is better suited for this system. Knowledge about the disturbance can be fed forward to the controller, and be taken into account before it occurs.

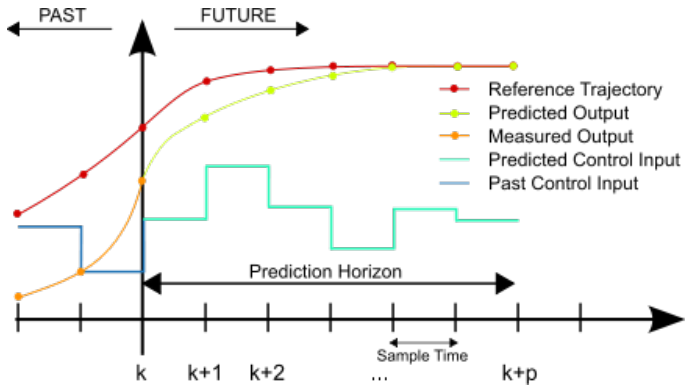

Figure 4.2: The figure shows the behaviour of the MPC

MPC is a relatively advanced control algorithm compared to the conventional control algorithms, such as PI and PID controllers. It uses a dynamic model of the process to predict future behaviour, and updates the controller once every time step, as can be seen in figure 4.2, based on a solution of a given optimization problem.

An advantage of the MPC is the ability to account for constraints in the system. A drawback of the controller is that the solving of the optimization problem is a heavy mathematical operation, and the algorithm is therefore computationally demanding. This is an area of research in this thesis.

Algorithm 4.1 Linear MPC with Output Feedback

for k=1,2,... **do**
Compute estimate of the state $\hat{x}_m$
Solve the Quadratic Programming (QP) problem with $\hat{x}_m$ as the initial condition
Apply the first control move $u_c(k) = u_c(k-1) + \Delta u$
end for

This chapter discusses the control system, including the API layer consisting of the MPC and the regulatory control layer comprising the Proportional-Integrator

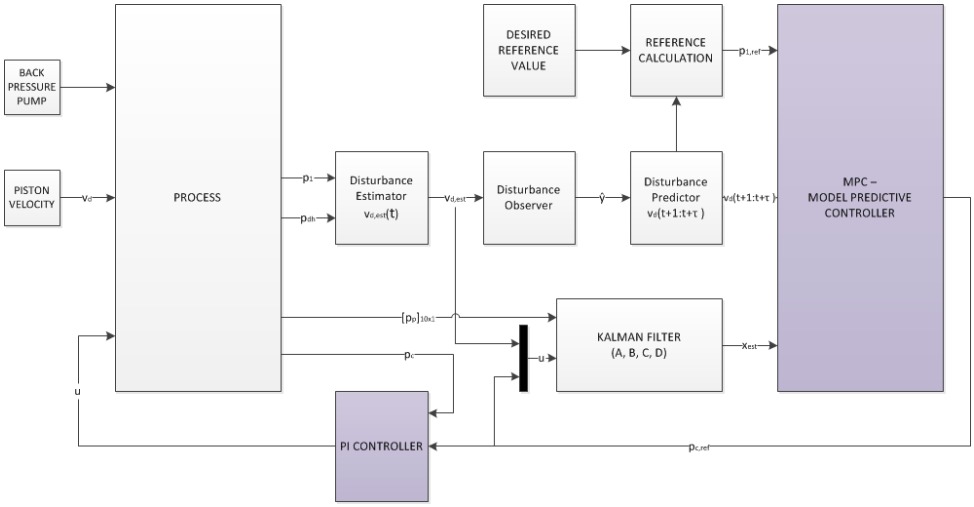

Figure 4.3: This figure gives a overview of the system, and the connection between the Kalman filter, the MPC, and the PI-controller.

(PI) controller. Figure 4.3 shows the coherence with the overall system. Algorithm 4.1 briefly explains the progress of how the MPC works.

4.1 The Optimization Problem

The MPC uses an optimization problem to achieve the desired performance of the control system. An example of an optimization problem can be to set up a fence around a field. The goal is to enclose as large as possible area of the field. A constraint is then the length of the fence.

The optimization problem can be approached from different angles, and two different approaches are discussed here. One is to refine a range the down-hole pressure is allowed to keep within, given by the constraints. A second approach is to keep the down-hole pressure inside the drilling window by setting a reference it should follow. In this section, these two methods are studied and discussed. In both cases, a model of the process used by the MPC is needed.

The MPC Model

In section 2.1, a model of the system is identified. Equation 2.1 shows the structure of the input and output to the model. The internal model of the MPC is based on

the black-box model, but the structure is changed, see equations 4.1-4.2.

$$\mathbf{x}_c(k+1) = \mathbf{A}_c\mathbf{x}_c(k) + \mathbf{B}_c\mathbf{u}_c(k) + \mathbf{E}_c d(k) \tag{4.1}$$

$$y_c(k) = \mathbf{C}_c\mathbf{x}_c(k) \tag{4.2}$$

Here, $u_c = p_c$ is the manipulated variable, $d = v_d$ is the disturbance, and $y_c = p_1$ is the CV. Equation 2.1 shows that the input to the process model is $\mathbf{u}_m = \begin{bmatrix} p_c \\ v_d \end{bmatrix}$. The elements in $\mathbf{B}_m = \begin{bmatrix} \mathbf{B}_{m,1} & \mathbf{B}_{m,2} \end{bmatrix}$ corresponds to each element in $\mathbf{u}_m$. This means that $\mathbf{B}_c = \mathbf{B}_{m,1}$ and $\mathbf{E}_c = \mathbf{B}_{m,2}$. The CV y_c coincides with the first element of $\mathbf{y}_m$. Thus $\mathbf{C}_c = \mathbf{C}_{m,1}$.

The model from chapter 2 is as mentioned earlier interpreted as deviation variables. Thus, the variables in the implementation of the MPC should be processed as deviation variables too.

4.1.1 The Constraint Method

The first approach to the optimization problem setup is to refine a small window for the down-hole pressure to vary within, rather than force it to follow a reference. In an engineering perspective, this is advantageous for several reasons. The periodically disturbance causes the pressure to oscillate periodically, thus the reference tracking controller needs to constantly make adjustments for the pressure to follow the reference. This leads to considerable wear of the choke, which is undesired. By defining a range the pressure can vary within, the controller will not be as eager in its adjustments as in the reference tracking setup, which is discussed in the next section. Figure 4.4 shows the connection between the reference trajectory and the drilling window. Besides the abrasion consideration, this approach is intuitive and easy to understand.

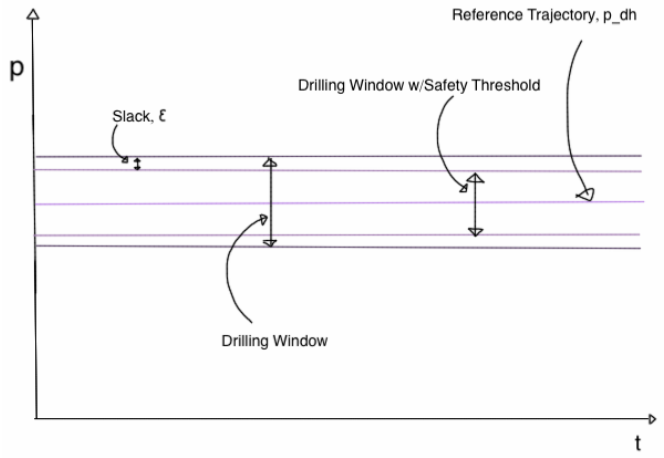

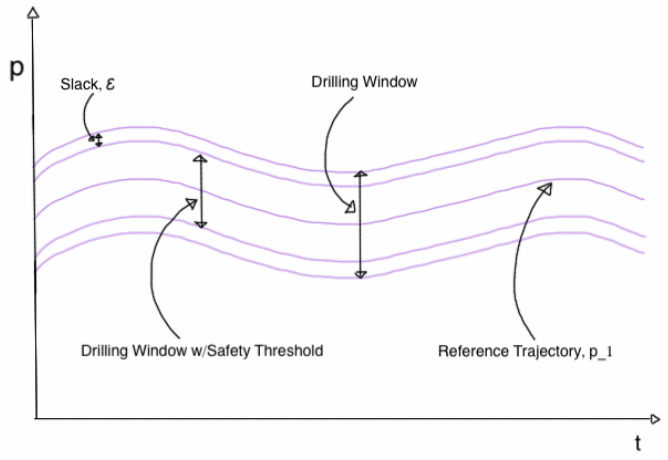

(b) p_1

Figure 4.4: The constraint method illustrated. The down-hole pressure reference, $p_{dh,ref}$, is constant. The drilling window, which it is desirable to keep within, is surrounding the reference trajectory (figure 4.4a). The corresponding drilling window for the CV is illustrated in 4.4a.

QP Problem Formulation

The constraint method setup does not aim to follow a reference trajectory. Therefore, the cost function emphasizes rate of change, $\Delta u_c(i) = u_c(i) - u_c(i-1)$, instead of the future trajectory, and the constraints gives a more narrow range for the pressure to vary within.

$$\min_u \ f(u, \varepsilon) = \sum_{i=1}^{k} \Delta u_c(i)^T \delta \Delta u_c(i) + \varepsilon(i)^T \gamma \varepsilon(i) \tag{4.3}$$

Subject to

$$\Delta u_L \leq \Delta u_c \leq \Delta u_U$$
$$-\varepsilon(i) + y_{c,L} \leq y_c \leq y_{c,U} + \varepsilon(i) \tag{4.4}$$

Here, $y_{c,L} = y_{c,ref} - \alpha$ and $y_{c,U} = y_{c,ref} + \alpha$, where 2α specifies the size of the drilling window with security threshold, which is shown in figure 4.4. The measure of deviation from the drilling window, ε, is implemented as an MV in order to minimize this deviation. In other words, f grows when the pressure exceeds the limitations.

4.1.2 Reference Tracking Method

The target of the second studied optimization problem setup is to attain a desired set point as effectively as possible. This is achieved by defining a cost function that penalizes deviation between the desired and the actual trajectory. The function is designed to find the optimal value of a MV to reach the set point. This optimal value should not cross the boundaries, or constraints, given by the system. If the constraints are violated, the problem becomes infeasible, see appendix A.2 for more details about feasibility.

QP problem formulation

The optimization problem is often a quadratic programming problem, QP problem, formulated as in equations 4.5-4.6. The weighting matrices Q, P, and S determine

the significance of the penalties given in order to attain the set point.

$$\begin{aligned}\min_u \ f(x,u) = &\sum_{i=0}^{k-1}\{(x_c(i)-x_{c,ref}(i))^T\mathbf{Q}(x_c(i)-x_{c,ref}(i)) \\ &+ (u_c(i)-u_{c,ref}(i))^T\mathbf{P}(u_c(i)-u_{c,ref}(i))\} \\ &+ (x_c(k)-x_{c,ref}(k))^T\mathbf{S}(x_c(k)-x_{c,ref}(k)) \end{aligned} \tag{4.5}$$

subject to

$$\begin{aligned} &x_{c,0} = given \\ &u_L \leq u_c(i) \leq u_U{}^1 \quad \text{for } 0 \leq i \leq k+1 \\ &y_L(i) \leq H_i x_i \leq y_U(i) \quad \text{for } 1 \leq i \leq k+1 \end{aligned} \tag{4.6}$$

$\mathbf{x}_c(i)$ is the i-th state of the system, and are the controlled variable in equation 4.5. $\mathbf{x}_{c,ref}(i)$ is the reference desired to follow. $u_c(i)$ is the MVs, commonly called the control variables.

4.2 Choice of Control Method

In this thesis, the control process is not a continuously ongoing process. It is a process which is only running during drilling, in relatively short periods of time. Thus, the wear of the choke is not a considerable concern. The choice of procedure is therefore a matter of preference. It is decided to go further with implementation of the reference trajectory MPC because there is more material available on this subject.

4.3 Rewriting the Optimization Problem

An optimization problem often needs to be customized to fit to each specific problem. In this case, it is desirable to control the down-hole pressure by changing the choke pressure. The down-hole pressure is not a part of the black-box model identified. Thus, equation 2.5 is used to map the desired pressure of the down-hole pressure to a corresponding pressure of p_1. Hence, the controlled variable in this problem is $y_c = p_1$, which is not a state, but an output from the system. It is therefore necessary to formulate the problem to optimize the output deviation rather than the state deviation. In addition, it is not reasonable to penalize the actual value of the control variable. It is no extra cost of applying a higher constant reference value. However,

[1] Remark that the lower and upper limits of u are constant, thus they are not denoted with index.

it is desired to keep the rate of change, Δu_c as small as possible. In other words, it is no extra cost associated with setting the choke position to 60 degrees than appling a 40 degree opening. Nevertheless, it is not desirable to change the position rapidly.

4.3.1 Integral Action

It is desirable to rewrite the system to include integral action to the MPC controller, by using the change of input as the MV, v, instead of the actual input variable. This is achieved by reformulating the system from equations 4.1-4.2 to the following:

$$\begin{aligned}\tilde{\mathbf{x}}(k+1) &= \begin{bmatrix}\mathbf{x}(k+1)\\ u_c(k)\end{bmatrix} = \begin{bmatrix}\mathbf{A}_c & \mathbf{B}_c\\ \mathbf{0} & \mathbf{I}\end{bmatrix}\tilde{\mathbf{x}}(k) + \begin{bmatrix}\mathbf{B}_c\\ \mathbf{I}\end{bmatrix}\Delta u(k) + \begin{bmatrix}\mathbf{E}_c\\ \mathbf{0}\end{bmatrix} d(k)\\ &= \tilde{\mathbf{A}}\tilde{\mathbf{x}}(k) + \tilde{\mathbf{B}}\Delta u(k) + \tilde{\mathbf{E}}d(k) \qquad (4.7)\\ y_c(k) &= \begin{bmatrix}\mathbf{C}_c & \mathbf{0}\end{bmatrix}\tilde{\mathbf{x}}(k) = \tilde{\mathbf{C}}\tilde{\mathbf{x}}(k) \qquad (4.8)\end{aligned}$$

Here, $\Delta u_c = u_c(k) - u_c(k-1)$. By inserting these system matrices into the problem formulation stated in the previous section, the MPC optimizes $\Delta u_c(i)$ instead of u_c.

In order to optimize with respect to the output y_c instead of the states, it is necessary to redefine the cost function. Equation 4.8 shows that $y_c(k) = \tilde{\mathbf{C}}_c\tilde{\mathbf{x}}_c(i)$. By rewriting the problem to equations 4.9-4.10, both the output optimization and the integral action are taken into consideration.

$$\begin{aligned}\min_u\ f(y,u) = &\sum_{i=0}^{k-1}\{(\tilde{\mathbf{C}}_c\tilde{\mathbf{x}}_c(i) - y_{c,ref}(i))^T Q(\tilde{\mathbf{C}}_c\tilde{\mathbf{x}}_c(i) - y_{c,ref}(i))\\ &+ \Delta u(i)^T P\Delta u(i)\}\\ &+ (\tilde{\mathbf{C}}_c\tilde{\mathbf{x}}_c(k) - y_{c,ref}(k))^T S(\tilde{\mathbf{C}}_c\tilde{\mathbf{x}}_c(k) - y_{c,ref}(k)) \qquad (4.9)\end{aligned}$$

subject to

$$\begin{aligned}&\tilde{\mathbf{x}}(0) = given\\ &\Delta u_L \le \Delta u(i) \le \Delta u_U \quad \text{for } 0 \le i \le k+1\\ &y_{c,L}(i) \le y_c(i) \le y_{c,U}(i) \quad \text{for } 1 \le i \le k+1 \qquad (4.10)\end{aligned}$$

Further, it is desirable to eliminate the summation sign. This is done by writing the states on matrix form as shown in appendix B, equations B.1-B.3. In the same way, the system matrices are stacked to fit into the problem formulation.

From this, it is possible to write the optimization problem as follows:

$$\min_{\mathbf{Y},\mathbf{v}} \begin{bmatrix} \mathbf{Y} \\ \mathbf{v} \end{bmatrix}^T \begin{bmatrix} \bar{\mathbf{Q}} & \mathbf{0} \\ \mathbf{0} & \bar{\mathbf{P}} \end{bmatrix} \begin{bmatrix} \mathbf{Y} \\ \mathbf{v} \end{bmatrix} \tag{4.11}$$

Subject to

$$\begin{bmatrix} \mathbf{I} & \mathbf{0} \\ -\mathbf{I} & \mathbf{0} \\ \mathbf{0} & \mathbf{I} \\ \mathbf{0} & -\mathbf{I} \end{bmatrix} \begin{bmatrix} \mathbf{Y} \\ \mathbf{v} \end{bmatrix} \leq \begin{bmatrix} \mathbf{Y}_U - \mathbf{Y}_{ref} \\ -\mathbf{Y}_L + \mathbf{Y}_{ref} \\ \mathbf{U}_U \\ -\mathbf{U}_L \end{bmatrix} \tag{4.12}$$

Here, there are $n_y + n_{\Delta u}$ optimization variables. To decrease the computation time, the superposition principle can be applied to reduce the number of optimization variables to $n_{\Delta u}$.

4.3.2 Reducing the Number of Optimization Variables

The future state trajectory is expressed by equation 4.1. As explained above, the control variable is Y, thus it is required to look at the future output trajectory instead of the state trajectory. The future output trajectory may be expressed as follows:

$$\mathbf{Y} + \mathbf{Y}_{ref} = \bar{\mathbf{C}}\bar{\mathbf{A}}\tilde{\mathbf{x}}_0 + \bar{\mathbf{C}}\bar{\mathbf{B}}\mathbf{v} + \bar{\mathbf{C}}\bar{\mathbf{E}}\mathbf{d} \tag{4.13}$$

See appendix B for the definition of the system matrices $\bar{\mathbf{A}}, \bar{\mathbf{B}}, \bar{\mathbf{C}}$, and $\bar{\mathbf{E}}$. By using the superposition principle, equation 4.13 can be divided into two parts, one dependent of the manipulated variable $\mathbf{v}$ and one independent of $\mathbf{v}$:

$$\mathbf{Y}_{dev} = \bar{\mathbf{C}}\bar{\mathbf{A}}\mathbf{x}_0 + \bar{\mathbf{C}}\bar{\mathbf{E}}\mathbf{d} - \mathbf{Y}_{ref} \tag{4.14}$$

$$\mathbf{Y}_{\mathbf{v}} = \bar{\mathbf{C}}\bar{\mathbf{B}}\mathbf{v} \tag{4.15}$$

$\mathbf{Y}_{dev}$ denotes the deviation from the desired output trajectory from equation 4.1 and $\mathbf{Y}_v$ denotes the effect of the MV on the future state trajectory. The above results in the optimization problem in equations 4.16-4.17. As can be seen, the number of optimization variables is now reduced to $n_{\Delta u}$.

$$\min_{\mathbf{v}} f = \frac{1}{2}\mathbf{v}^T\tilde{\mathbf{H}}\mathbf{v} + \mathbf{c}^T\mathbf{v} \tag{4.16}$$

Subject to

$$\mathbf{L}\mathbf{v} \leq \mathbf{b} \tag{4.17}$$

where

$$\tilde{\mathbf{H}} = \bar{\mathbf{B}}^T \bar{\mathbf{C}}^T \bar{\mathbf{Q}} \bar{\mathbf{C}} \bar{\mathbf{B}} + \bar{\mathbf{P}}$$
$$\mathbf{c}^T = \mathbf{Y}_{dev}^T \bar{\mathbf{Q}} \bar{\mathbf{B}}$$
$$\mathbf{L} = \begin{bmatrix} \bar{\mathbf{B}} \\ -\bar{\mathbf{B}} \\ \mathbf{I} \\ -\mathbf{I} \end{bmatrix}, \quad \mathbf{b} = \begin{bmatrix} \mathbf{Y}_U - (\bar{\mathbf{C}}\bar{\mathbf{A}}\tilde{\mathbf{x}}_0 + \bar{\mathbf{C}}\bar{\mathbf{E}}\mathbf{d}) \\ -\mathbf{Y}_L + (\bar{\mathbf{C}}\bar{\mathbf{A}}\tilde{\mathbf{x}}_0 + \bar{\mathbf{C}}\bar{\mathbf{E}}\mathbf{d}) \\ \Delta\mathbf{U}_U \\ -\Delta\mathbf{U}_L \end{bmatrix}$$

4.3.3 Solving the QP Problem

In order to solve the QP problem stated above, an algorithm called *active set* is used. The name *active set* describes a condition $C(x) \leq 0$ of an inequality constraint and is defined as follows:

- The condition is *active* if x is such that $C(x) = 0$
- The condition is *inactive* if x is such that $C(x) > 0$

The following pseudo-code shows the functionality of the active-set algorithm used to solve the QP problem in the controller.

Algorithm 4.2 Active-set algorithm to solve the QP problem

```
while not optimal enough solution do
    Solve the equality problem defined by the active set
    Compute the Lagrange multipliers of the active set
    Remove a subset of the constraints with negative Lagrange multipliers
    Search for infeasible constraints
end while
```

The Matlab function *quadprog* handles the QP problem solving. The solver analyses the feasibility of the solution, and finds the optimal CV of the problem. Feasibility is discussed in appendix A.2.

4.3.4 Convexity of the QP problem

The solution of the QP problem gives the optimal solution, the MV which minimizes the cost function. To ensure an optimal solution, the cost function must be a convex function and the feasible set[2] must be a convex set[3].

A QP problem is defined as a quadratic cost function with linear constraints. This means that the function is convex if Q is a symmetric, positive semi-definite matrix. Since all the constraints are linear, the feasible set is convex. Hence, the solution is optimal if Q satisfies the above requirement. See [6] for a comprehensive paper on the topic.

4.3.5 Control Input Blocking

Control input blocking is a method to save computational time in the solving of the QP problem which divides the prediction horizon of MVs into blocks. As can be seen from figure 4.5, the number of predicions are reduced. In computationally demanding problems where the aim is to reach a constant reference, this can be beneficial.

In this thesis, it is not advisable to implement blocking in the MPC. The reference trajectory is periodic due to the waves, thus it is not advantageous to use the blocking method.

[2]Feasibility are discussed in appendix A.2.
[3]Convexity is defined in appendix A.1

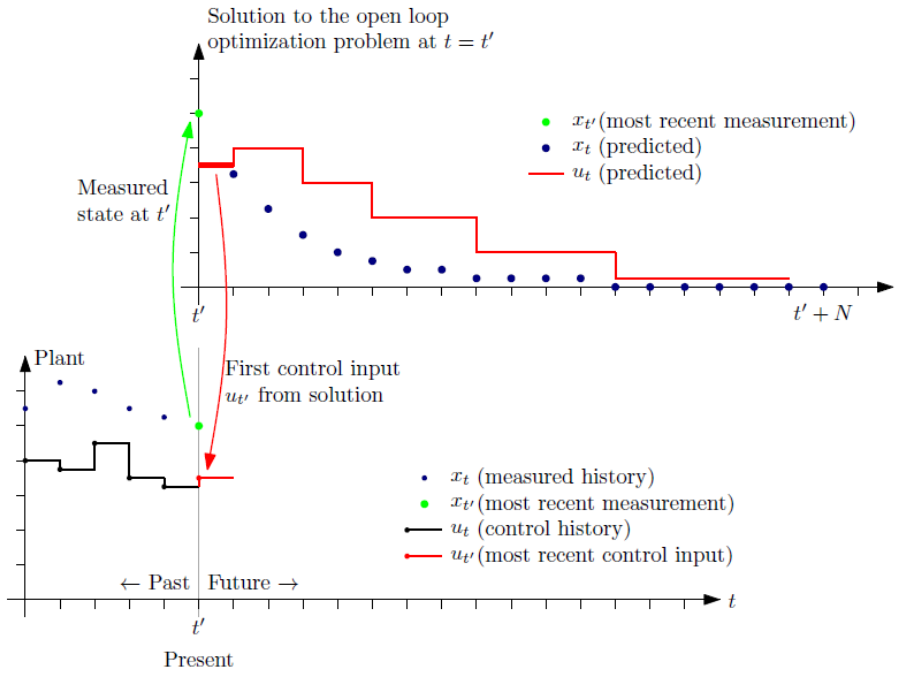

Figure 4.5: This figure shows the concept of control input blocking. The figure is obtained from lecture notes[6].

4.4 The Regulatory Control

When the MPC has calculated a set-point for the choke pressure, it is necessary to have lower level controllers to control the process to the set-point given from the APC layer. A PI-controller is used as an underlying controller of the MPC. Figure 4.3 shows the controller and its relationship to the rest of the control system.

4.4.1 The PI-controller

The PI-controller is as mentioned a proportional-integral controller, and is described mathematically as follows:

$$u_{PI}(t) = MV_{PI}(t) = K_p e(t) + K_i \int_0^t e(\tau) d\tau \tag{4.18}$$

where e is the difference between the CV, the set-point for the choke pressure p_c, and the measured choke pressure. K_p is the proportional gain, while K_i is the integral

gain. These specifies the impact of the controller, and are tuned for performance. The tuning is done experimentally, and can be a source of error. A poorly tuned controller can do more harm than good, hence the controller tuning requires some work. In addition, the tuning have an impact on the runtime of the controller. It is necessary that the dynamics of the regulatory control layer is faster than the dynamics of the APC-layer.

The process takes the opening of the choke in percentage as input, thus it is necessary to map the output to a choke opening setpoint. In addition to make the choke pressure follow the desired setpoint, the PI-regulator are supposed to handle the mapping. Equation 4.19 states the characteristics, where u is the choke opening.

$$G(u) = q_c\sqrt{\frac{\rho}{p_c - p_0}} \tag{4.19}$$

Inverting this and insertion of the desired choke pressure instead of the measured choke pressure leads to a non-linear expression of the choke opening:

$$u = G^{-1}(q_c\sqrt{\frac{\rho}{p_c - p_0}}) \tag{4.20}$$

The PI-regulator implementation was done by Anders Albert in the spring of 2013. In the fall of 2013, the controller was reviewed. Although the choke characteristics are well studied, it turned out that a PI-controller with a look-up table that mapped the reference choke pressure to a choke opening gave a more precise control. Thus, the PI-controller with look-up table as shown in appendix C was used. See Albert's Master's thesis[1] for additional details about the implementation.

4.5 Nominal Experiments

In the nominal tests, the model derived in chapter 2 is used as process. This is the same model used in the controller itself, and gives perfect conditions for the controller. Waves with different periods, from 3 to 10 seconds, are applied. In addition to the MPC performance, the Kalman filter and the disturbance observer are tested. Results can be seen in section 7.3.1.

Chapter 5
MPD Simulator

5.1 The Simulator

After running the nominal experiments of the MPC, it is tested against an MPD-simulator. The simulator was developed by Ole Morten Aamo and reviewed in the spring of 2013 by Jussi Mikael Ånestad[11]. It is based on a mathematichal model describing the IPT Heave Lab[1], and implemented as a function block in Matlab©. The simulator, shown in figure 5.1 allows the user to specify input parameters and provides output parameters from this, see table 5.1 for details about each parameter. The sketch of the lab in figure 6.1 shows the placement of each element in the lab.

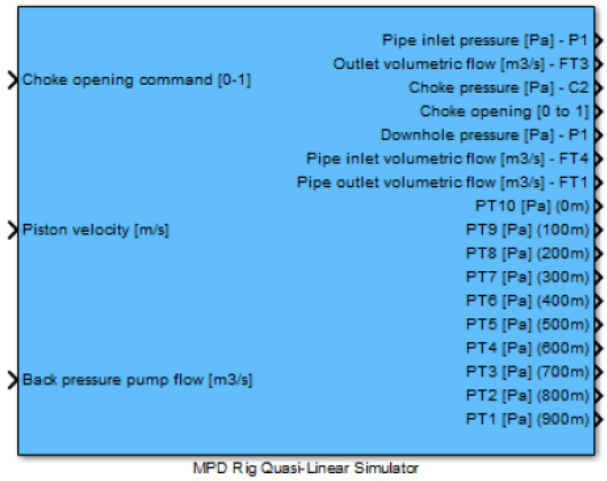

Figure 5.1: The simulator block from Matlab©, developed by Ånestad in the spring of 2013.

[1]The IPT Heave Lab is discussed in chapter 6.

Parameter Name	Symbol	Unit	Description
Input Parameters			
Choke Opening Command		0-1	The choke opening ordered, 0 is shut and 1 is fully opened
Piston Velocity		m/s	The velocity of the piston, called the disturbance
Back Pressure Pump flow		m^3/s	The flow from the back pressure pump into the system
Output Parameters			
Pipe Inlet Pressure	P1	Pa	Pressure in the inlet of the pipe
Outlet Volumetric Flow	FT3	m^3/s	Flow in the outlet of the well
Choke Pressure	C2	Pa	Pressure at the choke
Choke Opening	*	[0-1]	The actual choke opening
Downhole Pressure	P1	Pa	Pressure in the well, downhole
Pipe Inlet Volumetric Flow	FT4	m^3/s	Flow in the inlet of the pipe
Pipe Outlet Volumetric Flow	FT1	m^3/s	Flow in the outlet of the pipe
Pipe Pressure	PT1-PT10	Pa	Pressure nodes along drillstring, where PT10 is the node closest to the choke and PT1 closest to the downhole pressure node[2].

Table 5.1: Description of the parameters in the simulator.

5.2 Experiments With The Simulator

The simulator is developed to emulate the behavior of the IPT Heave Lab, thus it is reasonable to test the controller performance with the simulator as process before testing it in the lab. These tests are conducted with wave periods between 3 and 10 seconds, and with a back pressure pump rate of 32 $^{m^3}/_s$ to resemble the maximum flow rate in the lab.

The PI controller is adjusted to the lab and is therefore conservatively tuned. This precaution is due to real-time aspects, to ensure that the controller is sufficiently fast. In simulations, this is not a concern. Thus, it is adjusted to achieve optimal results, regardless of the resulting runtime. This optimizes the PI controller's performance significantly.

[2]Remark that the notation PT1-PT10 in the simulator block in figure 5.1 differs from the description. This is due to wrong notation in the simulator interface relative to the implementation.

Chapter 6
IPT Heave Lab

6.1 Brief Introduction

The IPT Heave Lab is a model of a connection scenario during drilling from a floating rig. The lab installation is a collaboration between the Department of Petroleum Engineering and Geophysics, NTNU, and Statoil, and simulates a vertical well 4000 meters deep. The lab is scaled down, and consists mainly of a 900 meters long coiled copper pipe connected to the choke by a rubber pipe, the BHA, and a back-pressure pump. Figure 6.1 shows a schematic setup of the lab, and the symbols correspond to table 5.1. For a more detailed documentation, see [1] and [5]

A Simulink© diagram is designed to handle measurements from the lab, and to apply the desired signals. It converts the signals to voltage and vice versa, and communicates with the sensors through a control card. Two electrical motors are controlling the choke valve and the piston movements, and communicate with the computer through a set of inverters.

In addition to the communication, the diagram ensures safety by stopping simulations if the pressure exceeds certain limits. The lower limit is set to -0.5 bar, which prevents vacuum to occur in the system. The upper limit is set to 10 bars.

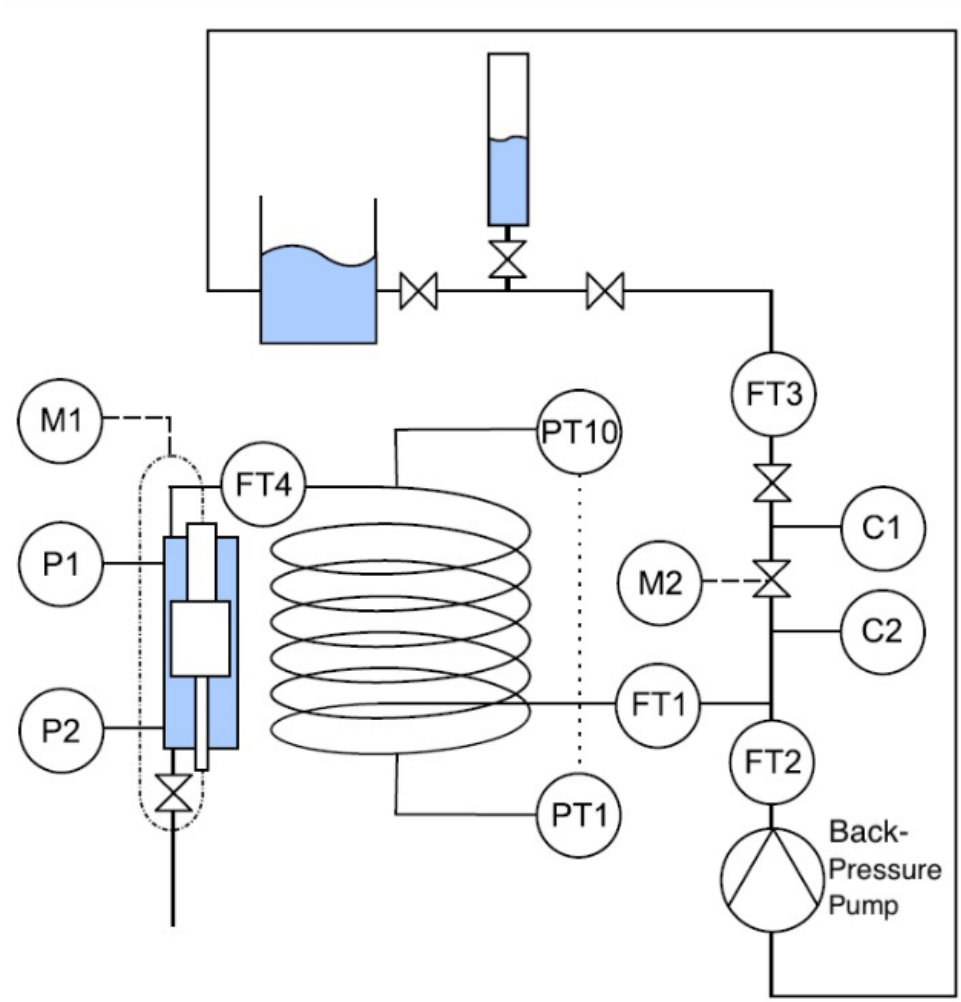

Figure 6.1: Sketch of the lab

6.2 Lab Preparation

In order to test the MPC controller in the lab, some alterations must be conducted. These are discussed in the following section.

6.2.1 Model Identification

A new model based on experimental data collected in the lab must be created. Data was obtained from the lab, and the identification process described in chapter 2 was conducted for these data. This model was adjusted and implemented into the system, i.e. the Kalman filter and the MPC matrices were changed.

6.2.2 Real-Time Aspects

It was assumed that the MPC controller runtime would exceed the real-time aspect of the lab. The MPC can be down-sampled to decrease the computational load. In addition, the model dimension can be decreased by not including all the pressure measurements in the model identification. This is discussed more thoroughly in section 7.1.1.

6.3 Experiments In The Lab

By performing tests of the control system in the lab, both the observer design and the controller performance are examined. The disturbance estimator is tested under imperfect conditions, in contradiction to the nominal tests. Experiments with different wavelengths and magnitudes are planned.

The experiments could not be conducted as planned, as problems with the setup occurred. These are discussed in section 7.3.4, and suggestions for changes to avoid the problems are presented in chapter 8.

Chapter 7
Results and Discussion

In the previous chapters, several testing scenarios for the MPC are described. In addition, a process model is derived, while observers are discussed and implemented. This chapter presents and discusses the results.

7.1 Model Identification Results

By performing system identification using black-box approximation, the results vary based on the choice of mathematical order. All orders up to 30 were tested. The choice of order was based on the deviation between the test-set output and the model output. As mentioned above, the goal was to obtain a mathematical model that generates output-data as close to the test-data as possible. The deviation between the model and test-set output should also not exceed an upper limit of a given threshold of 2.5 bar per measurement, since it is desirable to keep the drilling window as narrow as possible. As well as minimizing the model deviation, it is desirable to choose the lowest possible order because the computational runtime is dependent of the order.

As previously mentioned, it is not necessarily advantageous to include all the pressure measurement nodes in the model identification. The top pressure node in the drill string, p_{10}, has almost the exact same dynamics as the choke pressure, p_c. It was therefore decided to remove p_{10} from the model identification, and the identified model has 9 measurements instead of 10, as shown in equation 2.1. It can further be considered whether more pressure nodes should be removed.

The sampling time of the process model is crucial to the result. The model is sampled every 0.01 seconds, which is sufficient to obtain an adequate model. An

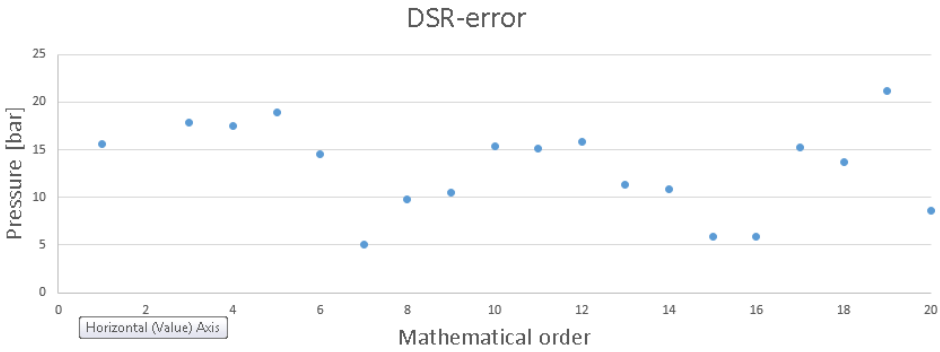

Figure 7.1: This figure shows the RMSE between the output of the test set and the model output.

incrementation of the sampling time leads to a less accurate process model.

By examining the results, the approximation using 20 as the maximal order and a mathematical order of 7 showed to be a reasonable choice, where the sum of the error is approximately 5 bars. This corresponds to an average error per measurement node of 0.55 bars. A model of order 12 and of maximal order 26 gives the smallest deviation between the process and model output, with a deviation of 4.3 bars, approximately 0.48 bars per measurement. Nevertheless, the model of order 7 is the favorable choice considering the trade-of between accuracy and complexity.

Figure 7.1 shows the total RMSE for models of order 1 to 20, with a maximal order of 20. It is clear that order 7 is the best choice. By comparing the model with the simulator, it was seen that p_1 was the node with the largest deviation. Figure 7.2 shows the deviation between the measurement of p_1 and the model estimate using a step from 50% to 60% opening in the choke opening. In the first 20 seconds, a stationary deviation can be seen. Here, the system is further from the working point, thus the model is less accurate. The oscillations at 0 and 20 seconds are caused by the sudden change in the choke opening.

7.1.1 Discussion Of The Identified Model

The results show that a model with 7 states is able to model a process with 9 outputs. From this, it can be argued that it is insufficient dynamics in the system to justify the number of outputs in the identification. By including redundant parameters in

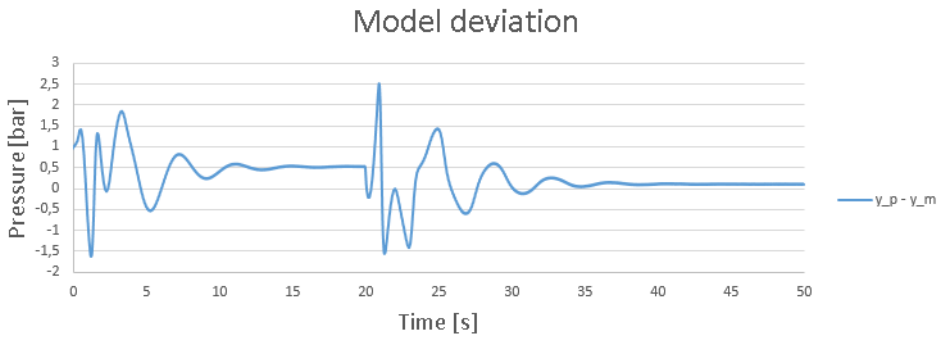

Figure 7.2: This figure shows the deviation between the measured pressure $p_1 = y_p$ from the process and the modeled pressure y_m.

the model, over-parametrization occurs. This leads to excessive computational load and should be avoided.

7.1.2 Review of Identification from Project Work

In the project work from the Fall 2014 [4], a pure black-box model of the system was identified, with the following inputs and outputs:

$$u_m = [p_c \; v_d]^T \tag{7.1}$$

$$y_m = [p_1 \; p_2 \; p_3 \; p_4 \; p_5 \; p_6 \; p_7 \; p_8 \; p_9 \; p_{10} \; p_{dh}]^T \tag{7.2}$$

When reviewing the project work, several major errors in the implementation was found. Thus the model identification was redone based on the same identification data in order to obtain an equitable basis for comparison.

The theoretical changes done with the model identification from the project work [4] are the known output $\mathbf{Y}$. p_{dh} is no longer a part of the black-box approximation. Figure 7.3 shows that the best model is created by using the mathematical order of 9, with maximal order of 26[1]. The sum of error was approximately 6 bars ≈ 0.55 bars per measurement. This is the same deviation as the new model. Nevertheless, the total model error is smaller, assuming that the known dynamics used in the gray-box model are more accurate. In addition, the model order is higher for the pure black-box model than for the gray-box model. Thus, it can be concluded that

[1]Remark that there is no point for the 2. and 26. pressure node deviations in figure 7.3. The reason for this is that the deviations were very large, and did not fit into the graph.

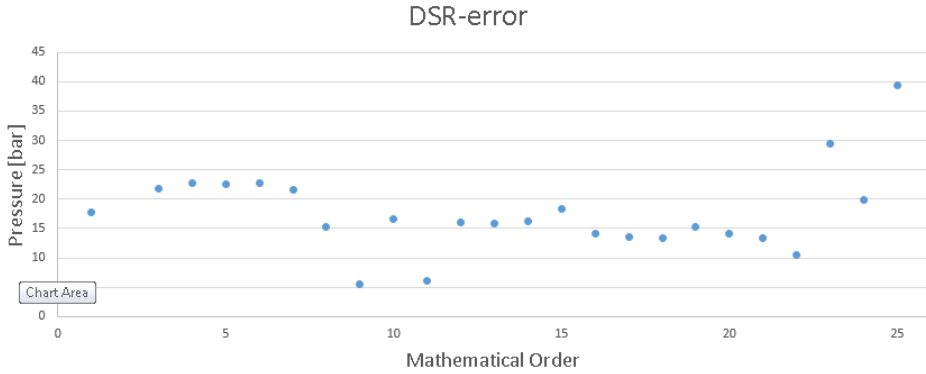

Figure 7.3: This figure shows the RMSE between the output of the test set and the model output from the model identification done in the project work from the Fall of 2013 [4].

the gray-box model is a better representation of the system than the pure black-box model.

7.1.3 Model Identification In The Heave Lab

A model of the Heave Lab was derived based on experimental data collected in the lab. Here, a similar evaluation of the results as above were done. Moreover, a model of order 13 was created. During the implementation of the Kalman filter, conversion of the model from discrete-time to continuous-time was necessary, using Matlab© function *d2c*. Throughout the conversion, negative real poles were found in the model, thus a state was added. This caused a problem with the dimensions of the system relative to the Kalman gain found by the *dsr*-algorithm. Difficulties arose as a result of this, thus it is limited amount of results from the lab, showed in section 7.3.4.

7.2 Observer Design

This section handles the results of the disturbance prediction and the ability of the Kalman filter to produce state estimates.

7.2.1 Disturbance Estimator

Simulator Results

Chapter 3 concerns the estimation and prediction of the disturbance. It is of interest to examine the accuracy of this prediction. In the simulator, the relationship between p_1 and p_{dh} is modeled by equation 2.5, thus the estimate $\hat{v}_d$ was assumed to be correct. Figure 7.4 shows that the estimate is identical to the actual disturbance, as anticipated.

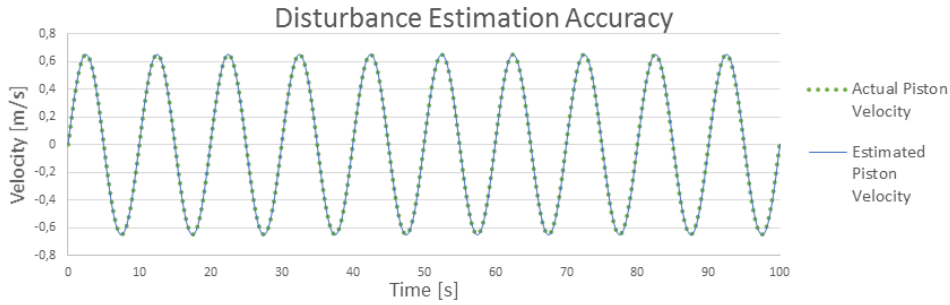

Figure 7.4: This figure shows the accuracy of the disturbance estimator.

Lab Results

The disturbance estimator and observer were tested in the lab. Here, the conditions were not perfect, unlike the previous case. As can be seen in figure 7.5, the estimate deviated considerably from the actual piston velocity. The reason for this is assumed to be that the pressure does not propagate in the same manner in the lab as in the simulator. In other words, the parameters in equation 2.5 does not give an adequate description of the down-hole dynamics in the lab, and need to be tuned.

The equation parameters identified by Aanestad [11] need to be reviewed in order to improve the disturbance estimate. The parameters require tuning, which in this case is done by examining the pressure propagation in terms of the piston velocity. In the experimental lab, this measurement can be obtained. However, it is unavailable

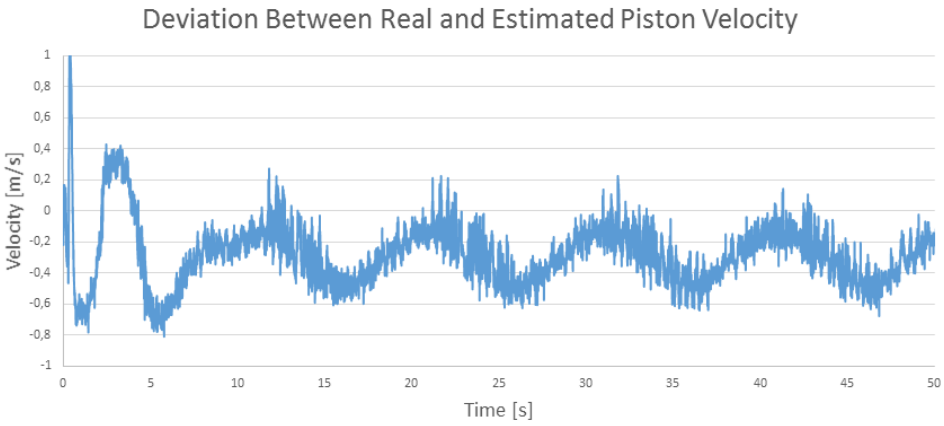

Figure 7.5: This figure shows the accuracy of the disturbance estimator illustrated by the deviation between the real and the estimated piston velocity, $v_d - \hat{v}_d$.

in practical applications, and the tuning of the parameters may be challenging. Consequently, it is desirable to find another solution to the tuning problem.

A method to avoid the bias in the estimated disturbance is to add an offset. By looking at the steady-state case of equation 2.5, the pressure difference between p_{dh} and p_1 should be equal to the hydrostatic pressure, ρgh. By adjusting the equation to fulfill this, the bias is eliminated. It is suggested as a point in further work to examine this relationship.

7.2.2 Kalman Filter

During the nominal tests of the Kalman filter, the state of both the process (x_m) and the estimated state ($\hat{x}_m$) were available. These were compared, and found to be identical. Since the process model was the same as the process, this was as anticipated.

During simulator experiments, the process state was not available, and comparison was unattainable. However, the filter performance was evaluated by looking at the output deviation $y_p - y_m$. Figure 7.6 shows the deviation between the real and the estimated output of pressure node p_1. As the figure shows, the deviation is significant, which indicates that the filter have a potential of improvement.

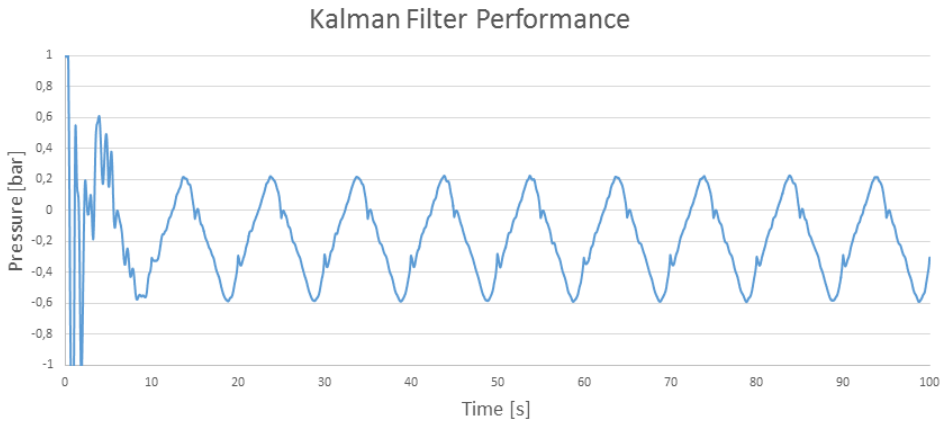

Figure 7.6: This figure illustrates the performance of the Kalman filter. The graph shows the deviation between the process output and the estimated output from the kalman filter, $y_p - y_m$. Only pressure node p_1 is plotted.

7.3 Controller Performance

7.3.1 Results of Nominal Experiments

Several nominal[2] tests were conducted, showing good performance of the controller. The figures 7.7-7.8 show the controller's ability to reject waves with amplitude 0.65 meters and period of 10 and 3 seconds, respectively.

Figure 7.7: The disturbance rejection of waves with a period of 10 seconds.

Waves With Period Of 10 Seconds

The results above show that the controller is able to reject the wave disturbance when it contains a feed-forwarding, as illustrated by the blue graph. The green graph shows the pressure when the disturbance is not feed-forwarded. From this, it is clear that the pressure change due to the vertical movement of the piston is greatly suppressed, from an amplitude of approximately 5 bars to 1 bar. This corresponds to an 80% reduction of the wave impact.

Moreover, the controller ensures that the pressure follows the reference pressure value, which is represented by the orange graph.

[2]A nominal test in this case is testing of the controller with the model of the process as the controlled process, i.e. the same model as the internal model in the MPC.

Waves With Period Of 3 Seconds

In the slightly more demanding case, where the period of the waves was 3 seconds, the pressure oscillation amplitude was decreased from approximately 4.5 bars to 1.2 bars, which is a reduction of about 73%.

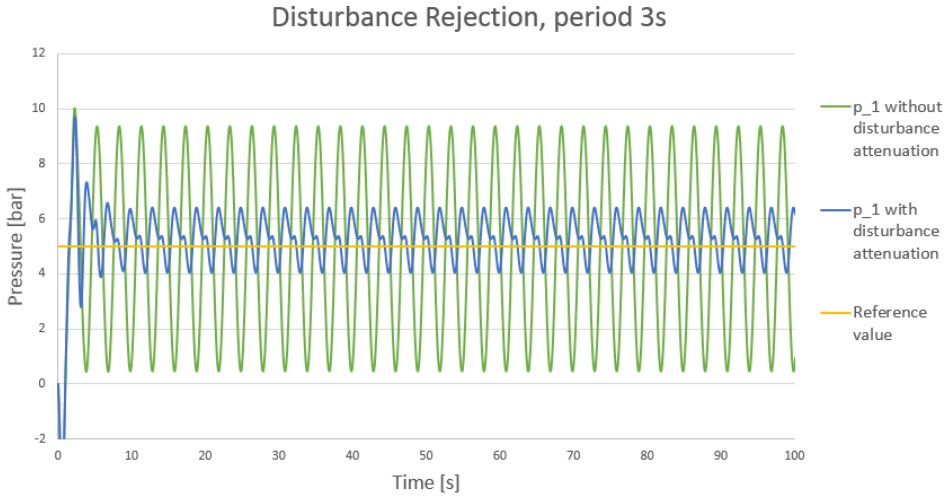

Figure 7.8: The disturbance rejection of waves with a period of 3 seconds.

Weighting

The MPC controller was tuned during the initial tests, and the weights in equation 7.3 showed to be the preferred choice.

$$\begin{aligned} &\text{Weight on } \Delta u(i) = P = 2000 \\ &\text{Weight on } y_c(i) - y_{c,ref}(i) = Q = 2000 \\ &\text{Weight on } y_c(k) - y_{c,ref}(k) = S = 4000 \end{aligned} \tag{7.3}$$

7.3.2 Results from Simulator Experiments

By testing the controller system against the simulator, the ambient was more realistic than in the nominal tests. The process model is not exactly the same as the simulator model, thus the testing scenario is more arduous. It is expected that the results from the simulator tests are less successful.

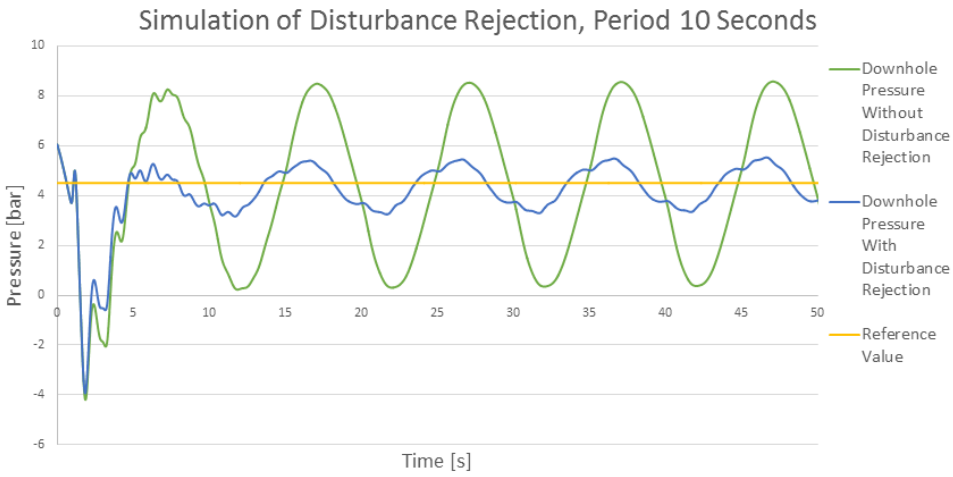

Figure 7.9: The disturbance rejection of waves with a period of 10 seconds, simulator test.

Waves With Period Of 10 Seconds

By comparing figure 7.7 and 7.9, it can be seen that the wave motion has greater effect on the process model than the simulator, i.e. the amplitude of the pressure oscillations is higher in the nominal tests. This is a model error, which can lead to errors in the regulation of the process.

From figure 7.9, it is clear that the disturbance rejection was quite successful. The waves of 10 seconds period was attenuated effectively, and the amplitude of the pressure oscillations were reduced from about 4 bars to about 1 bar. This is a reduction of 75%, 5% lower than in the nominal test.

Waves With Period Of 3 Seconds

In the case of waves of 3 seconds period, the disturbance is rejected to a lesser extent than in the previous case. The amplitude of the pressure oscillation is reduced from approximately 4 bars to 1.5 bars, decreased with 63%.

7.3.3 Discussion Of Results

In the previous sections, the results from the nominal experiments and the simulator tests were presented. It is clear from these tests that it is more attainable to suppress

Figure 7.10: The disturbance rejection of waves with a period of 3 seconds, simulator test.

the impact of waves with longer period. The propagation time of the wave effect can be a reason for this. In the process model, the propagation is taken into account automatically, since the experimental data includes these properties. However, rapid changes in pressure are harder to suppress.

The controller suppressed the disturbance in a greater extent under perfect conditions in the nominal tests, as anticipated. The wave impact is 5% more suppressed in the nominal test compared to the simulator test with 10 seconds period, similarly 10% in the 3 seconds period case.

Sources of Error

In the nominal tests, the sources of error should be few. The weighting matrices are not necessarily optimal, as these were found by trial and error.

The simulator tests are more realistic than the nominal tests, thus more sources of error occur. The process model is not an exact description of the process. This can easily be seen by comparing figure 7.7 and 7.9. The heave motion causes a larger amplitude in the pressure oscillations in the simulator than in the process model.

The PI controller is not able to follow the desired pressure reference the MPC controller requests exactly. This causes a deviation between the ordered choke pressure and the actual choke pressure, which leads to a less accurate regulation of the down-hole pressure. However, the deviation is minor in the simulation experiments. The deviation $p_{c,ref} - p_c$ can be seen in figure 7.11. Even though the lab experiment

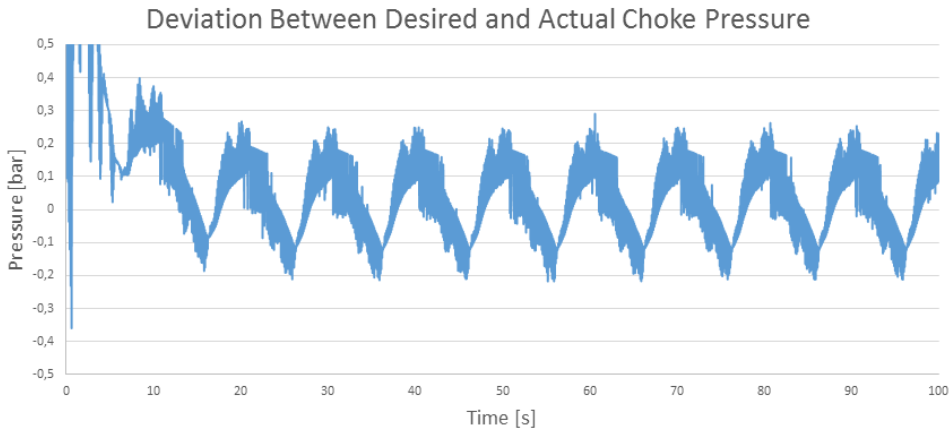

Figure 7.11: The deviation between the reference choke pressure and the actual choke pressure indicates the performance of the PI controller. This figure shows the deviation in a case with waves of period 10 seconds.

results are limited, the PI controller were expected to perform less accurate in that case. The gain can not be tuned aggressively in the lab, because the runtime would have exceeded the real-time, and the problem would become infeasible.

Another source of error that can be seen in figure 7.11 is the noise in the system. The origin of this noise is believed to be the PI controller. This is clear from exploration of the plots of p_c and $p_{c,ref}$ separately, which are not remarkably noisy.

7.3.4 Results and Discussion from Lab Experiments

MPC experiments were not successful in the IPT Heave lab. In the process of making the continuous Kalman filter, the Matlab© function *d2c()* was used[3]. This function found that the model contained a real negative pole, and replaced this pole with a pair of complex conjugate poles, and thus increased the model order. The Kalman gain is calculated from the *dsr* algorithm, and is of the original order of the system.

[3]For more information about the function, see [8].

Thus, the Kalman filter matrices and the gain do not match in dimensions. Because of this, the MPC controller performance was not examined.

The problem with order incrementation could be avoided by developing a time-discrete Kalman filter. Theory from [3] and the procedure of developing the discrete filter were examined. However, due to lack of time, the implementation was not completed.

The lack of results from the MPC controller tests in the lab makes it hard to compare the results from this thesis with previous work. Anders Albert [1] achieved a 46% suppression of the heave motion from waves of period 3 seconds in the lab. The results from the simulator experiments indicate a good performance of the MPC controller. However, these results are not comparable to Alberts lab results, and it is impossible to consider whether the controller performance is improved.

Chapter 8
Conclusion and Future Work

8.1 Conclusion

8.1.1 Model Identification

The model identification conducted in chapter 2 was successful, and the black-box model was improved compared to the model from the project work[4]. This was clear from the reduced order of the model, and a decreased overall model error.

The modification in the model identification was to remove two pressure measurements in the model identification, p_{10} and p_{dh}. p_{10} has nearly the same dynamics as the choke pressure p_c, thus it is unnecessary to include it in the identification.

The number of measurements in the model identification exceeds the mathematical order of the optimal model describing the process. This raises questions concerning over-parameterization. Over-parametrization leads to unnecessary computational load, which should be avoided.

The known non-linearities describing the down-hole dynamics were utilized. Thus, the down-hole pressure measurement was removed from the black-box model identification. This is assumed to improve the model further. The white-box model uses two measurements from the well. Thus, it is required to measure p_1.

8.1.2 Observer Design

The disturbance estimator worked as anticipated in the simulator tests. Equation 2.5 is used in the description of the down-hole dynamics both in the estimator and the simulator, thus the estimate was expected to be correct.

In the IPT Heave Lab, the estimate of the disturbance was significantly less accurate. This might be caused by different pressure propagation in the lab compared to the simulator. Tuning of the parameters in equation 2.5 may increase the accuracy of the estimates, and thus improve the performance of the disturbance observer. There are suggested several procedures to the tuning process in section 8.2.

8.1.3 Controller Performance

The MPC controller was implemented and the results from the nominal tests and the simulations were positive. The down-hole pressure managed to follow the reference value, and the disturbance was attenuated. A reduction of the wave impact of as much as 80% in the nominal tests, and 75% in the simulator tests was satisfactory. However, it is unreasonable to compare the simulator test results with the previous work on the matter since no lab results of the MPC controller performance from this thesis were obtained.

It was observed that the PI controller introduced noise to the system in the simulations. Moreover, it was a deviation between the real and the desired reference. This was not noticeably in the simulator experiments, however it is expected to be less satisfying in the lab due to tuning considerations.

8.2 Future Work

8.2.1 Review Number Of Measurements Needed

As can be seen from the results of the model identification, the number of measurements was higher than the number of states in the optimal process model. This indicates that the model is over-parametrized, and that the model dimension, and consequently the runtime, can be decreased by reducing the number of measurements in the identification. An example is to include every other measurement in the drill-string.

8.2.2 Tuning of the Disturbance Estimator

The performance of disturbance estimator in relation to the lab is discussed. It is necessary to adjust equation 2.5 to ensure estimation accuracy. The parameter tuning may be performed by considering equation 2.5 with the known disturbance from the lab. On the other hand, the disturbance is assumed unknown, and the

tuning may be done without this measurement by adding a bias calculated from steady-state calculations.

8.2.3 Improvements of the Kalman Filter

In order to avoid the problem discussed in section 7.2.2 that occurred in the Kalman filter, a possible solution are suggested. A discrete-time Kalman filter can be used. This should be achievable to obtain, and would not affect the performance noticeably if the sampling time is reasonable.

8.2.4 Avoid The PI Controller

As mentioned in the results, the PI controller is a relatively extensive source of error in the system. An alternative model identification can be performed, where the choke opening replaces the choke pressure as an input. By doing this, the CV in the controller is the choke opening, which can be applied direct to the process. This setup completely eliminates the PI controller, and avoids a considerable source of error.

References

[1] Anders Albert. Disturbance attenuation in managed pressure drilling. Master thesis, NTNU, June 2013.

[2] Steve Devereux. *Drilling Technology in Nontechnical Language*. PennWell Books, 2012.

[3] David Di Ruscio. Combined Deterministic and Stochastic System Identification and Realization: DSR - A Subspace Approach Based on Observations. *Modeling, Identification and Control*, 17(3):193–230, 1996.

[4] Siri Garli Dragset. Disturbance attenuation in managed pressure drilling. Project work, NTNU.

[5] Robert Drønnen. Disturbance generation in an experimental lab setup for managed pressure drilling. Master thesis, NTNU.

[6] Bjarne Anton Foss and Tor Aksel N. Heirung. Merging optimization and control. Lecture Notes, 2013.

[7] Svein Olav Hauger. Mpc - model predictive control. Lecture Notes, 2013.

[8] Mathworks. The d2c function, 2014.

[9] Mathworks. The quadprog function, 2014.

[10] Mathworks. Write level-2 matlab s-functions, 2014.

[11] Jussi Mikael Ånestad. System identification and simulation of an experimental setup for managed pressure drilling. Master thesis, NTNU.

[12] J. Nocedal and S. J. Wright. *Numerical Optimization*. Springer, New York, 2nd edition, 2006.

[13] Official Magazine of the International Association of Drilling Contractors. Mpc opens door to new well control options in deepwater, 2013.

Appendix A

Theorems and Definitions

A.1 Convexity

In [12, p. 8], convexity of both sets and functions are defined. A *set* is convex if it is possible to draw a straight line between two arbitrary points inside the set. In the same way, a *function* is convex if the straight line drawn between two arbitrary points on the function lies above the function itself. Figure A.1 illustrates this:

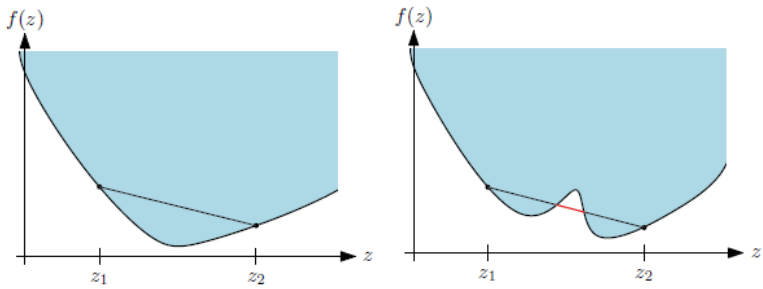

(a) A convex function. **(b)** A non-convex function.

Figure A.1: Figure A.1a shows a convex function, and figure A.1b shows a non-convex function. Figure obtained from lecture notes[6].

Defined more formally, a set $S \in \mathbb{R}^n$ is convex if the following holds: for $x \in S$ and $y \in S$, $\alpha x + (1-\alpha)y \in S$ for all $\alpha \in [0,1]$.

A function f is convex if

$$f(\alpha x + (1-\alpha)y) \leq \alpha f(x) + (1-\alpha)f(y) \quad \text{for all } \alpha \in [0,1] \tag{A.1}$$

A.2 Feasibility

The term *feasible set* refers to the set of points in an optimization problem which satisfies its constraints. If the solution of the optimization problem lies in this set, the problem is called *feasible*. Feasibility can be checked mathematically, but it is decided to take an experimental approach in this thesis. The Matlab© function used to solve the QP problem, *quadprog()*, sets an exit-flag describing the exit condition of the function. Feasibility of the QP problem in this thesis is ensured by looking at this exit-flag. For more information about this function, see [9] for additional information about the *quadprog()* function.

Another aspect of the feasibility problem is the real-time aspect. This concerns the capacity of running the program written in real-time in the lab. This is crucial in order to obtain reasonable data from the lab. If the computational time exceeds real-time, the controller will not be able to convey data in time.

Appendix B

QP Problem Formulation, Details

In order to reduce the problem to equation 4.11, the states are stacked into the following matrices:

$$\mathbf{Y} = \begin{bmatrix} y_c(1) - y_{c,ref}(1) \\ y_c(2) - y_{c,ref}(2) \\ \vdots \\ y_c(n) - y_{c,ref}(n) \end{bmatrix}, \quad \mathbf{Y}_{ref} = \begin{bmatrix} y_{c,ref}(1) \\ y_{c,ref}(2) \\ \vdots \\ y_{c,ref}(n) \end{bmatrix}$$

$$\mathbf{v} = \begin{bmatrix} v(0) \\ v(1) \\ \vdots \\ v(n-1) \end{bmatrix}, \quad \mathbf{d} = \begin{bmatrix} d(0) \\ d(1) \\ \vdots \\ d(n-1) \end{bmatrix}, \quad \Delta u_{ref} = 0 \tag{B.1}$$

Here, $v(i) = \Delta u(i)$. The weighting matrices are expressed as follows:

$$\bar{Q} = \begin{bmatrix} Q & 0 & \cdots & 0 & 0 \\ 0 & Q & \cdots & 0 & 0 \\ \vdots & \vdots & \ddots & \vdots & \vdots \\ 0 & 0 & \cdots & Q & 0 \\ 0 & 0 & \cdots & 0 & S \end{bmatrix}, \quad \bar{P} = \begin{bmatrix} P & 0 & \cdots & 0 & 0 \\ 0 & P & \cdots & 0 & 0 \\ \vdots & \vdots & \ddots & \vdots & \vdots \\ 0 & 0 & \cdots & P & 0 \\ 0 & 0 & \cdots & 0 & P \end{bmatrix} \tag{B.2}$$

Likewise, the constraint matrices are written as follows:

$$\Delta\mathbf{U}_L = \begin{bmatrix} \Delta u_L \\ \vdots \\ \Delta u_L \end{bmatrix}, \quad \Delta\mathbf{U}_U = \begin{bmatrix} \Delta u_U \\ \vdots \\ \Delta u_U \end{bmatrix}, \quad \mathbf{Y}_L = \begin{bmatrix} y_L \\ \vdots \\ y_L \end{bmatrix}, \quad \mathbf{Y}_U = \begin{bmatrix} y_U \\ \vdots \\ y_U \end{bmatrix}, \tag{B.3}$$

In equation 4.13, the matrices are defined as follows:

$$\bar{\mathbf{A}} = \begin{bmatrix} \tilde{\mathbf{A}} \\ \tilde{\mathbf{A}}^2 \\ \vdots \\ \tilde{\mathbf{A}}^n \end{bmatrix}, \quad \bar{\mathbf{B}} = \begin{bmatrix} \tilde{\mathbf{B}} & \mathbf{0} & \cdots & \mathbf{0} \\ \tilde{\mathbf{A}}\tilde{\mathbf{B}} & \tilde{\mathbf{B}} & \cdots & \mathbf{0} \\ \vdots & \vdots & \ddots & \vdots \\ \tilde{\mathbf{A}}^{n-1}\tilde{\mathbf{B}} & \tilde{\mathbf{A}}^{n-2}\tilde{\mathbf{B}} & \cdots & \tilde{\mathbf{B}} \end{bmatrix} \tag{B.4}$$

$$\bar{\mathbf{C}} = \begin{bmatrix} \tilde{\mathbf{C}}_c & \mathbf{0} & \cdots & \mathbf{0} \\ \mathbf{0} & \tilde{\mathbf{C}}_c & \cdots & \mathbf{0} \\ \vdots & \vdots & \ddots & \vdots \\ \mathbf{0} & \mathbf{0} & \cdots & \tilde{\mathbf{C}}_c \end{bmatrix}, \quad \bar{\mathbf{E}} = \begin{bmatrix} \tilde{\mathbf{E}} & \mathbf{0} & \cdots & \mathbf{0} \\ \tilde{\mathbf{A}}\tilde{\mathbf{E}} & \tilde{\mathbf{E}} & \cdots & \mathbf{0} \\ \vdots & \vdots & \ddots & \vdots \\ \tilde{\mathbf{A}}^{n-1}\tilde{\mathbf{E}} & \tilde{\mathbf{A}}^{n-2}\tilde{\mathbf{E}} & \cdots & \tilde{\mathbf{E}} \end{bmatrix} \tag{B.5}$$

Appendix C

The PI Controller

Figure C.1 shows the implementation of the PI controller. The look-up tables are in the *Integral Gain*-block, and determines the magnitude of the integral gain. The saturation block ensures that the ordered choke opening never exceeds the physical upper limit of the choke[1], and it also specifies that the lower bound for the choke is an opening of 35 degrees. This lower limitation is set to avoid excessively high pressures in the well.

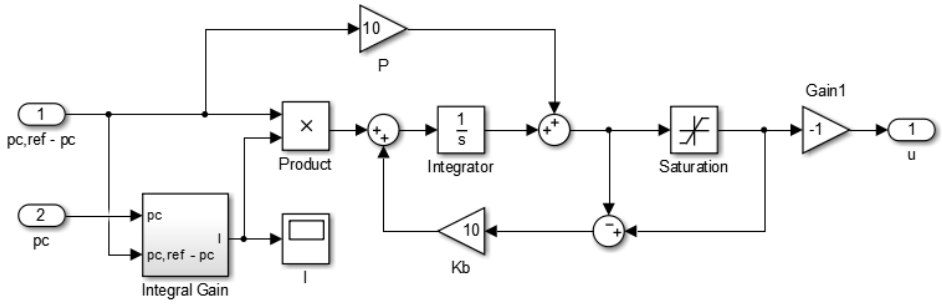

Figure C.1: This figure shows the implementation of the PI-controller.

[1]The choke is fully open at 90 degrees.

Appendix D
User Manual to Matlab Code

D.1 Model Identification

The experimental data is created by running the script *identification_data_generator.m*. The data files *ident_wp.mat* and *test_wp.mat* is created, which is used in the model identification. Remember to add the whole folder to the Matlab path.

To run the model identification, select and run the file *model_identification.m*. When finished, the order and the optimal maximal order is found and saved in the workspace, and the data file *dsr_error.mat* contains the RMSE for every possible combination of maximal orders and orders.

After running the model identification, a model of the desired order is created by specifying this and running the file *model_identification_single.m*.

D.2 Nominal Tests and Simulator Tests

To conduct the nominal tests, run the script *setup_mpc.m* from the folder MPC. Select the Simulink diagram *nominal_test_mpc.slx* and click run. The same applies to the simulator tests: run the script *setup.m*, and select the Simulink diagram *system_implementation.slx*. To change the reference value of the down-hole pressure, p_{dh}, simply change the value in the $p_{dh,ref}$ block in the Simulink diagram. To change the wave period, go to the script *setup.m* and change variable *period*.

D.3 IPT Heave Lab

To run the model identification with the experimental data from the lab, open the folder *Lab_Identification* and follow the same procedure as in section D.1.

Due to the problems occuring when running *setup_lab.m*, it was not done testing of the MPC in the lab. However, the Simulink diagram *interfaceIPT_0506_mpc.slx* is designed to run the lab tests. It was tested with a poor process model, and it ran without problems. Thus, it is possible to use this when a proper model is derived.